ERA report series

24 An ensemble of 20th century ocean reanalyses for providing ocean initial conditions for CERA-20C coupled streams

Eric de Boisséson and Magdalena Balmaseda

Series: ERA Report Series

A full list of ECMWF Publications can be found on our web site under:

http://www.ecmwf.int/en/research/publications
Contact: library@ecmwf.int

European Centre for Medium Range Weather Forecasts
Shinfield Park, Reading, Berkshire RG2 9AX, England

ABSTRACT

ORA-20C is a 10-member ensemble of ocean reanalyses covering the 20th century using atmospheric forcing from ERA-20C. Its main purpose is to provide initial conditions for the ocean component of the CERA-20C streams. One of the main uncertainties when conducting an experiment like ORA-20C is on the state of the ocean in the 1900s. Preliminary experiments were conducted to characterize the ocean model drift and the model response to time varying forcing and changes in the observing system. These experiments were used to provide an ensemble of ocean initial states for ORA-20C. ORA-20C shows a large spread in the first part of the century before the assimilation strongly constrains all the members toward an ocean state that is comparable with other reanalysis products. The ORA-20C reanalysis highlights the issues that need to be solved in order to provide a consistent 20th century ocean record. Dealing with the transition between the poorly observed early 20th century and the well-sampled later decades is a major challenge to take up before a product such as ORA-20C can be used for the detection of robust climate signals in the ocean subsurface. Treatment of model error is key to deal with changes of the observing system. A better bias correction algorithm may help constraining the solution in the first half of the century and stand as a concrete lead to explore.

I. Introduction

The first ERA-CLIM project led to the first European 20th century atmospheric reanalysis called ERA20C [*Poli et al*, 2016]. ERA-20C assimilates only conventional observations of surface pressure from the International Surface Pressure Database (ISPD) and marine winds from the International Comprehensive Ocean-Atmosphere Data Set (ICOADS). The second ERA-CLIM project is going further and at aims at producing a 20th century climate reanalysis called CERA-20C and based on the ECMWF coupled data assimilation system [*Laloyaux et al*, 2016]. This system couples the IFS to the NEMO framework and assimilates in parallel atmospheric and ocean observations.

Century reanalyses cannot be produced in a single stream because of computing cost and of time limitations. In that context, CERA-20C has to be run in several parallel streams. For each stream, the IFS component is initialised by ERA-20C while the NEMO component is initialised from a 20th century ocean data assimilation (ODA) run assimilating only temperature and salinity profiles from the EN4 dataset and with a Sea Surface Temperature (SST) nudging towards the monthly analysis from the Hadley Centre Sea Ice and Sea Surface Temperature data set version 2 (HadISST2). The production of this ODA run, called in the following ORA-20C (Ocean ReAnalysis of the 20th Century), is described in this document. A serious difficulty to deal with when conducting such an experiment is the uncertainty about the state of the ocean in the early 20th century due to the very poor observation coverage. The challenge is thus to produce an ocean analysis which will reflect such uncertainty while providing a sensible long-term record of the ocean state.

After a short description of the NEMO configuration, the NEMOVAR data assimilation system and the ocean boundary conditions in Section 2, this manuscript addresses the method used to spin up the ocean model in Section 3. In this Section, ocean runs conducted without data assimilation are analysed and issues related to initial conditions, model drift and parameterisation are addressed. Section 4 describes the data assimilation experiments used to provide a range of initial conditions reflecting the

uncertainty of the ocean state in 1900. Section 5 gives a detailed account of the production of an ensemble of 20th century ODA experiments, with a focus on climate signals, trends and outstanding issues. Section 6 summarizes and draws the conclusion of this work.

II. NEMO configuration and boundary conditions

1. NEMO configuration

NEMO model experiments are conducted on the ORCA1Z42 grid corresponding to a 1˚ horizontal resolution with a refined mesh in the tropics and 42 vertical levels with a first layer of 10 meters. NEMO includes the Louvain-la-Neuve Sea Ice Model (LIM) version 2 and active wave-ocean interactions using wave parameters from the atmospheric forcing [*Breivik et al*, 2015]. A relaxation to climatological Sea Surface Salinity (SSS) is applied to prevent issues in sensitive areas (next to sea-ice and runoff). In 20th century experiments, the ocean is forced by surface fields from ERA-20C at 3-hour frequency. SST and 3D relaxation are used in most of the experiments. In that case, the SST is nudged towards HadISST2 monthly analysis with a relaxation coefficient of $-200 W m^{-2}$ and a weak (20-year timescale) 3D relaxation to temperature and salinity climatology from the World Ocean Database [*Boyer et al,* 2009]. In assimilation experiments, EN4 temperature and salinity profiles [*Good et al*, 2003] are assimilated using the NEMOVAR system [*Mogensen et al*, 2012] with a 1-month window. The EN4 dataset is very sparse in the early 20th century and the number of observations starts to be substantial from the 1950s (Figure 1).

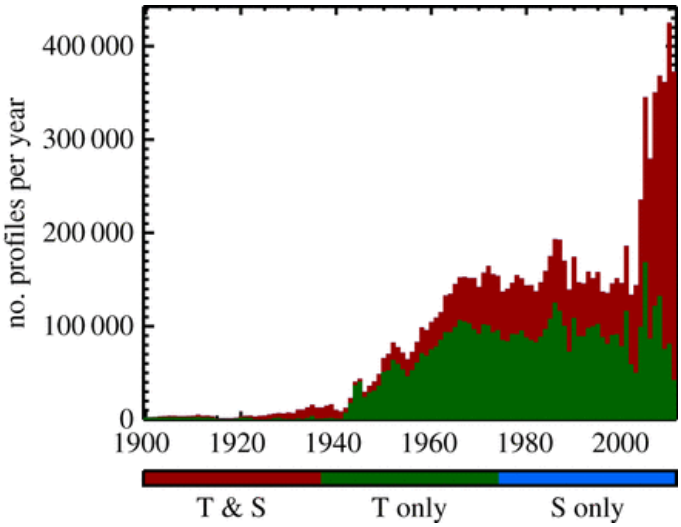

Figure 1 Annual evolution of the number of ocean profiles in the EN4 dataset. Temperature-only data are in green, just salinity-only in blue (too few to distinguish) and Temperature/Salintiy profiles are in red. Crown Copyright.

2. ERA-20C forcing and HadISST2 analysis

ERA-20C provides surface atmospheric parameters that combined with the ocean surface parameters in the bulk formula will produce the surface forcing fields. ERA-20C has already thoroughly been described in *Poli et al* [2015], but a few facts are repeated to support the discussion on the behaviour of the ocean model over the 20th century.

ERA-20C 2m temperature shows a large (about a degree) positive trend through the 20th century (Figure 2). Over the North Atlantic Ocean, the temperature is modulated by the Atlantic Multidecadal Oscillation while the Southern Ocean shows a clear change of regime from the first (colder) to the last decades (warmer) of the century. The change is particularly strong in the Atlantic and Indian sectors where it can reach +5K.

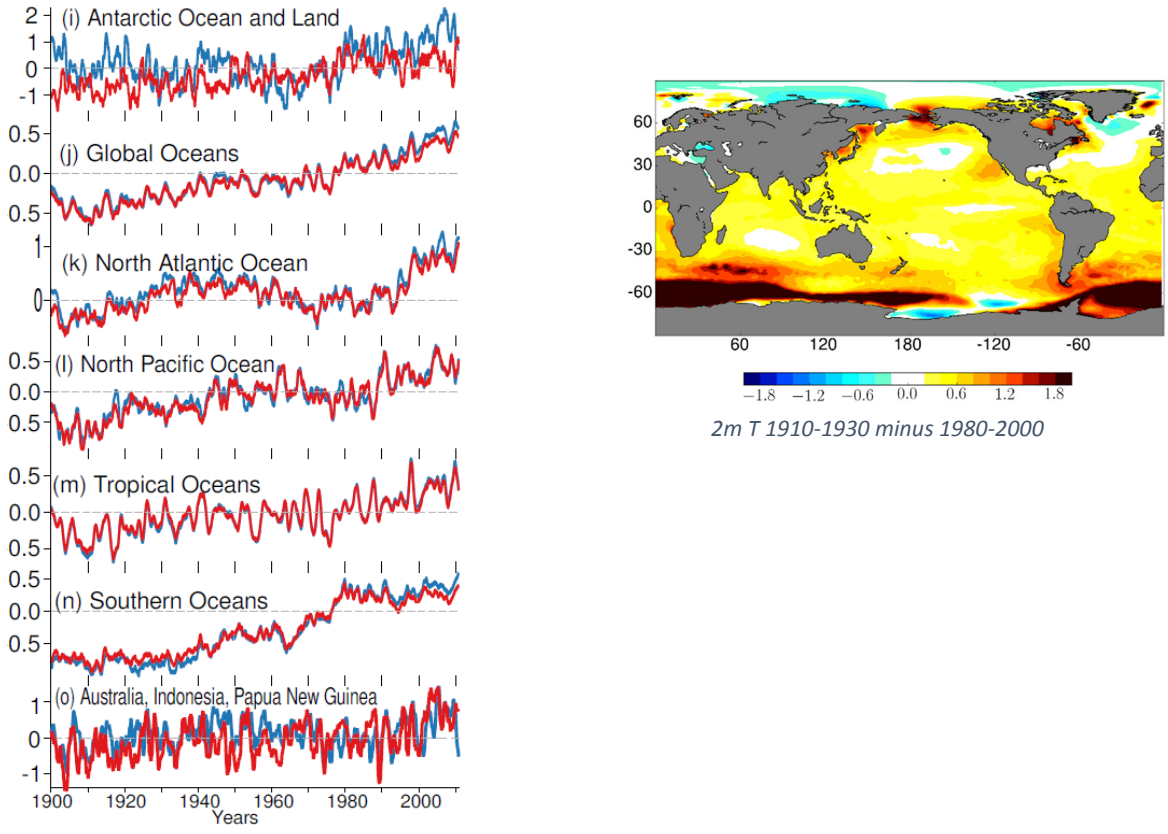

2m T 1910-1930 minus 1980-2000

Figure 2 (Left panel) Monthly anomalies for two-meter temperature from ERA-20C analyses (blue) and ERA-20CM (red) for various regional averages. Reference years for the climatologies are 1961–1990. 12-month movingaverage is applied. See Figure 18 from Poli et al [2015]. (Right panel) Change in two-meter temperature (in K) between the period 1910-1930 and 1980-2000 in ERA-20C deterministic. Colour saturates over the Southern Ocean with changes reaching 3K.

Global surface fluxes computed within ERA-20C shows a net thermal and heat flux loss towards the lower boundary from the 1970s but the surface net heat fluxes has interannual-to-decadal variability but no long-term trend (Figure 3)

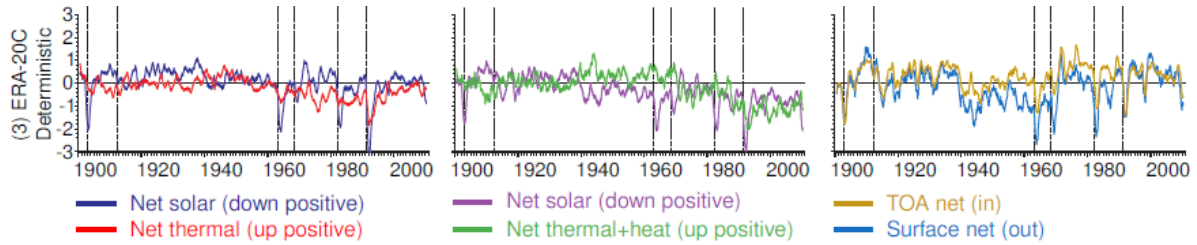

Figure 3 Evolution of the 12-month moving average of anomalies of energy budgets for ERA-20C deterministic, relative to years 1900–1909. The first column shows TOA net radiation fluxes for solar and thermal. The second column shows net surface fluxes for solar radiation, and thermal radiation plus latent and sensible heat. The third column shows TOA net total radiation flux (RT in gold) and surface net total flux (FS in blue). The vertical black dash linesindicate major volcanic eruptions (in chronological order): Santa Maria, Novarupta, Mount Agung, Fernandina Island,El Chich´on, and Pinatubo. From Poli et al. [2015] Figure 25.

Ensembles from the HadISST2 analysis have been used to force ERA-20C atmosphere. In ocean relaxation experiments, only the control member will be used for the SST relaxation. HadISST2 globally shows a continuous increase in temperature over the century particularly in the Southern hemisphere and in the North Atlantic (Figure 4). The only area showing a slight cooling is the subpolar North Atlantic in the Irminger and Labrador seas where deep convection is happening in winter.

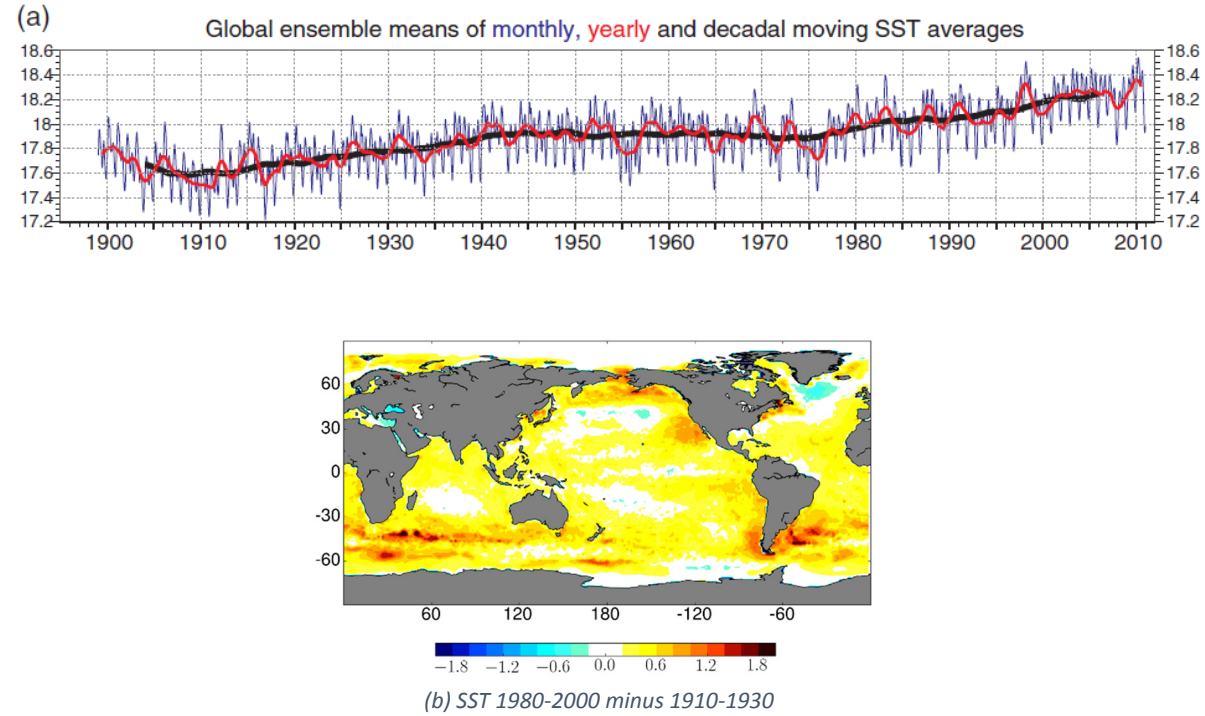

Figure 4 (a) Time series of HadISST.2.1.0.0 sea surface temperature (◦C) for global average of the SST ensemble mean (blue = monthly, red = yearly, black = decadal moving average). From Hersbach et al. [2015] Figure 1. (b) SST change (in K) between the periods 1980-2000 and 1910-1930.

III. Spin up experiments

A serious difficulty when conducting century long ocean simulations and reanalyses is the close to nil knowledge of the ocean state during the first half of the 20th century. We thus decided to initialise our first ocean experiments with an ocean state from 01/01/1979 taken from a previous ODA experiment using a similar setting as ORAS4 [*Balmaseda et al*, 2013] and forced by ERA-Interim fields [*Dee et al*, 2011]. The differences between the years 1900 and 1979 and the atmospheres from ERA-20C and ERA-Interim are very likely to induce a substantial spin-up or down of the ocean model. To explore this issue and the consecutive model drift, three different types of 20th century experiments are conducted - free model, relaxation and data assimilation experiments – and listed in Table 1. The purpose these experiments is to analyse the behaviour of the model and decide for an adequate spin-up strategy.

First, two free model experiments are run. The first one uses the time-varying ERA-20C forcing (FREE) while the second one loops over the year 1900 of ERA-20C (FREE-CST). The purpose of these experiments is to discriminate as much as possible the model drift from the variability linked to the forcing. Then, we conduct a relaxation (RLX) experiment starting from the same initial conditions as FREE, but using the SST and 3D relaxation as described in Section II.1. The aim is to capture a realistic SST mean state and variability with a strong SST constraint (about 3-day time scale). The 3D relaxation is much weaker (about 20-year time scale) and aims at limiting the drift in the ocean interior. The last experiment of this set is an assimilation run (ASM) similar to RLX (same initial conditions, same relaxation), but assimilating the EN4 T/S profiles. Comparison of ASM with RLX allows to identify the impact of assimilating ocean observations.

The experiments are compared in terms of time evolution of ocean and salt content, the spatial patterns of the trends. We also relate changes in the ocean heat content with changes in the Atlantic Meridional Overturning Circulation (AMOC).

1. Free model runs

In the FREE run, the global ocean heat content (Figure 5a,b,c) spins down, reaches a low plateau in the 1910-1930s and starts drifting with a large positive trend. The cooling during the first 10 years happens mainly in the upper 700m (1.e9 J/m2), with 0.6e9 in the upper 300m and 0.4e9 between 300m and 700m). The FREE-CST run shows a similar behaviour, without the interannual-to-decadal variability, and with slightly modified vertical distribution of heat (with a larger contribution from the depths below 700m). This indicates that a large part of the low frequency variability in FREE is due to model drift. Part of the differences between FREE and FREE-CST are indicative of the signal induced by the time varying forcing. In the total column heat content, differences arise mainly after 1970 (Figure 5c). For the period 1970-2010, the ocean in FREE warms at a rate of 1W/m2 faster than FREE-CST, which is larger than the ocean warming from other estimates (*Balmaseda et al,* 2013, *Levitus,* 2012).

Experiment	SST/3D Relaxation	Assimilation	Bias correction	Forcing	Initial conditions
FREE-CST	No	No	No	ERA-20C year 1900	ORAS4-like (fvsa) 19790101
FREE	No	No	No	ERA-20C	ORAS4-like (fvsa) 19790101
RLX	Yes	No	No	ERA-20C	ORAS4-like (fvsa) 19790101
ASM	Yes	Yes	No	ERA-20C	ORAS4-like (fvsa) 19790101
ANoBias	Yes	Yes	No	ERA-20C	RLX 19590101
ABias1	Yes	Yes	Yes (from ODA run forced by ERA-Interim)	ERA-20C	RLX 19590101
ABias2	Yes	Yes	Yes (from ODA run forced by ERA-20C)	ERA-20C	RLX 19590101
ORA-20C	Yes	Yes	No	ERA-20C with perturbations	Various ocean states from ANoBias, ABias1 and ABias2 (See Section V.1

Table 1 Configuration of the different NEMO and NEMOVAR experiments conducted in this study

Differences between the 1910-1930 low and the 1980-2000 high-heat-content-period are computed for both experiments, at the surface (Figure 6) and for different depth ranges (Figure 7). The FREE-CST (Figure 6a) experiment does not show any surface warming but a localized and intense cooling in the North Atlantic (Labrador and Irminger sea, and along the Western side of the basin), and along the path of the ACC. There is some localized warming by the Greenland and Norway Seas, and at the edge of the ACC in the Indian and Atlantic basins. Below the surface (0-700m, Figure 7a), the drift in FREE-CST is characterized by a prominent warming of the Tropical and South Atlantic and a cooling of the North Atlantic. There is also a weak warming in the South Pacific-Indian Ocean, poleward of the subtropical gyre. Below 700m (Figure 7c), the most striking feature is the intense warming around Antarctica and the cooling along the northern edge of the ACC, in the tropical Pacific and the Indian Ocean. The Atlantic basin exhibits the similar drift pattern as in the waters above, with more pronounced cooling in Eastern North Atlantic, and warming along the path of the Western Boundary Currents (WBC). The signature of the drift in the Atlantic basin is consistent with a reduction of the northward transport associated with a weaker AMOC (Figure 8). The dipole along the deep ACC (with warming to the south and cooling to the North) suggests the inability of the model to maintain a strong Polar Front, leading to the mixing of Antarctic Intermediate Water with the much colder Circumpolar Deep Water. This can also explain the deep cooling in Tropical Pacific /Indian, which can result from the poleward transports of colder waters.

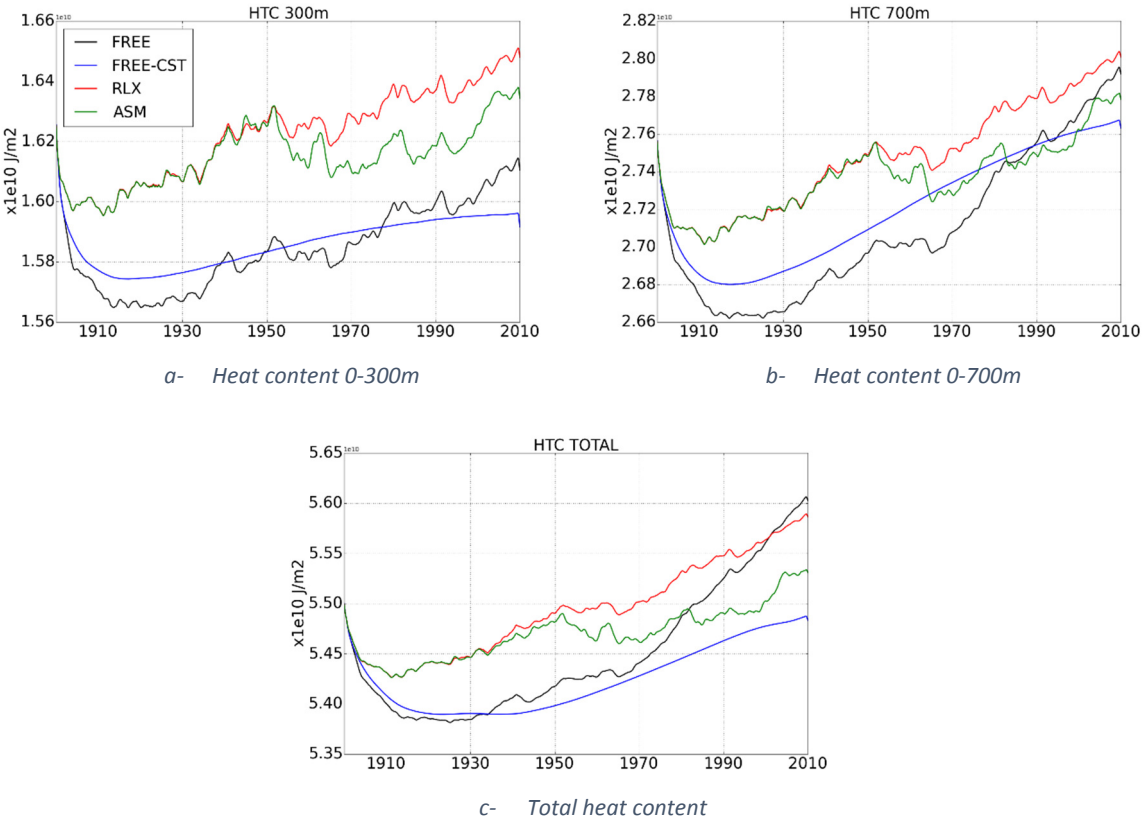

a- Heat content 0-300m

b- Heat content 0-700m

c- Total heat content

Figure 5 Evolution of the global ocean heat (in Jm^{-2}) content for the layers (a) 0-300m, (b) 0-700m and (c) 0-bottom. The FREE experiment is in black, FREE-CST in blue, RLX in red and ASM in green.

The patterns of ocean heat content change in FREE (Figure 6b and Figure 7b,d) are largely similar to those of FREE-CST, as expected from an evolution dominated by the model drift, but there are also some notable differences. Experiment FREE shows a surface warming driven by the time varying surface forcing. The SST globally increases except for the North Atlantic and Pacific basins and off Antarctica (the Ross Sea) in the Pacific Ocean (Figure 7b). The North Atlantic cooling is even stronger and more extensive than in experiment FREE-CST and also higher than in HadISST2 and in the 2-meter temperature from ERA-20C (Figure 2 and Figure 4b). The cooling in the North Pacific is absent in FREE-CST and in HadISST2, and it is likely induced by the increased vertical mixing of heat associated with time varying winds. The warming at the surface is consistent with this idea (Figure 7b). The waters below 700m in experiment FREE show similar pattern as in FREE-CST, but with weaker amplitude, except for the warming along the WBC and the Tropical Atlantic, which appears stronger in FREE (Figure 7d).

To sum up, the model drift is characterised by i) a cooling and freshening (see Supplementary materials for salinity plots, Figure 23) in the North Atlantic extending from the top to the deep ocean, particularly in areas of mode water formation and deep convection and ii) a warming and a gain of salt in the Equatorial and South Atlantic. This suggests a lack of meridional exchanges in the Atlantic basin both at the surface and at depth. The AMOC at 26˚N indeed collapses passing from 16Sv at the beginning of the run to values lower than 5Sv from the 1970s onwards (Figure 8). On the one hand, the amount of warm and salty waters transferred in the upper layers from the Tropics to the subpolar Atlantic is thus substantially reduced. On the other hand, water masses in the Irminger and Labrador Seas are continuously fed by cool and fresh water coming from the sea ice melting

without being efficiently advected southward in the deep branch of the AMOC. This lack of meridional transfer of water masses is likely to be due to common ocean model issues with vertical mixing and/or with the behaviour of the sea-ice model exporting too much ice.

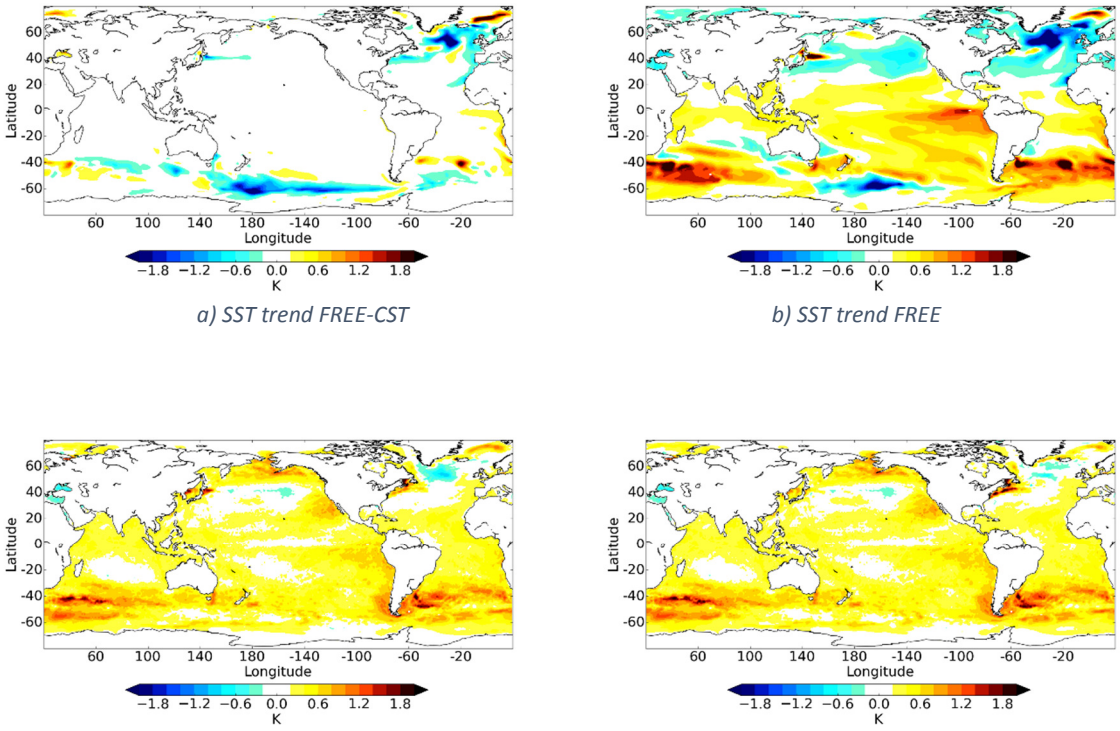

a) SST trend FREE-CST

b) SST trend FREE

c) SST trend in RLX

d) SST trend in ASM

Figure 6 Difference between the periods 1980-2000 and 1910-1930 in SST (in K) in experiments a) FREE-CST, b) FREE, c) RLX and d) ASM.

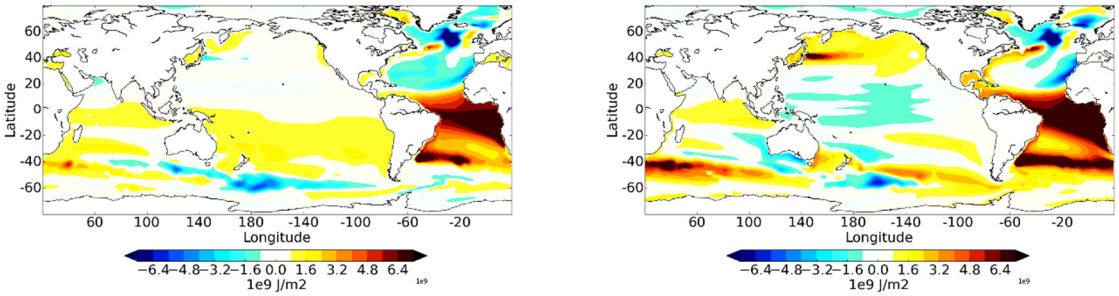

a) HC 0-700m trend FREE-CST *b) HC 0-700m trend FREE*

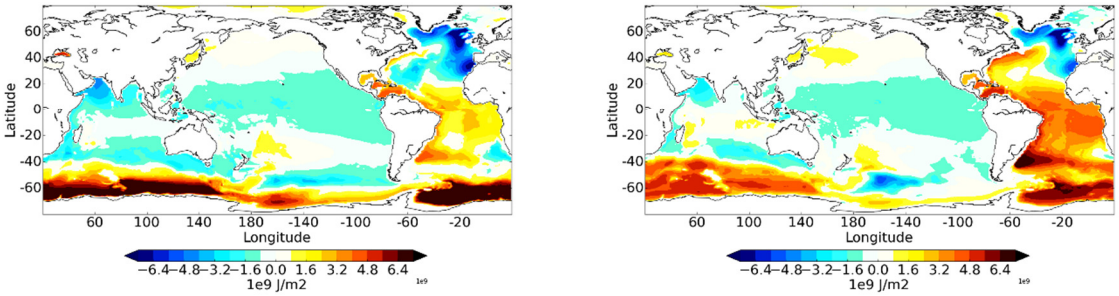

c) HC 700-btm trend FREE-CST *d) HC 700-btm trend FREE*

Figure 7 Difference between the periods 1980-2000 and 1910-1930 in a,b) heat content (in Jm^{-2}) for the 0-700m and c,d) heat content for depths below 700m for the FREE-CST and the FREE experiments, respectively.

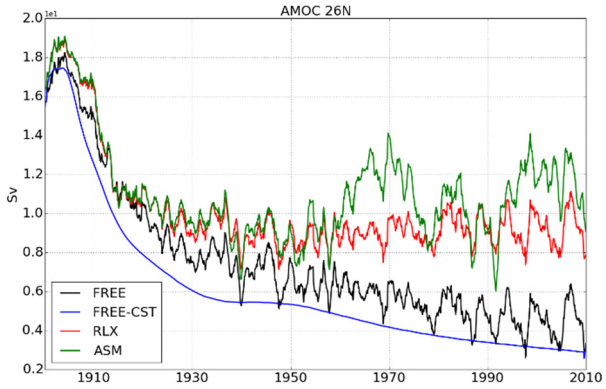

Figure 8 Intensity of the AMOC at 26N in Sv for the FREE (black), FREE-CST (blue), RLX (red) and ASM (green) experiments.

2. Relaxation and assimilation runs

The free model runs are useful as they will help understanding part of the behaviour of the relaxation and assimilation experiments that are constrained by observations.

In the relaxation run (RLX), the spin-down of the global ocean heat content is much reduced when compared to FREE (Figure 5a,b,c) and values stay relatively high over the 1910-1930 period. While the 0-300m layer shows a similar trend as in FREE, the large positive trends seen in the deeper layers after the 1910-1930's low are substantially reduced. The ocean heat content from the assimilation run (ASM) is matching well RLX in the poorly-observed first half of the 20th century. Once the observation coverage is good enough to have an impact, the post-50s trend in heat content seen in RLX is damped in ASM, which allows distinguishing the interannual variability signals.

The SST trend in RLX and ASM is very similar to the one from HadISST2 as a result from the SST relaxation (Figure 6c,d to compare with Figure 4b). In deeper layers (Figure 9a,c), the same dipole pattern seen in FREE in the Atlantic Basin is present in RLX but with much weaker intensities. This weakening is due to the 3D relaxation that warms the upper 1000m of the North Atlantic while cooling the Tropical and South Atlantic basins (Figure 10a,b,c). In ASM, the subsurface (0-700m) heat content increase in the equatorial and south Atlantic is further reduced. A strong gain of heat coincides with the Gulf Stream and a dipole warming/cooling in the Atlantic subtropical and subpolar gyres, respectively, extends to the bottom (Figure 9b,d). The 3D relaxation in ASM has the same impact as in RLX in the first part of the century (Figure 10d,e,f). Then the increment is taking over, reducing the intensity and the impact of the relaxation (Figure 10g,h,i). The upper ocean warming seen in the North Pacific in FREE (Figure 7b) is not visible in RLX and ASM (Figure 9a,b) as a result of the observational constraint. Below 700m, the gain of heat content in south Atlantic is greatly reduced in RLX and even disappears in ASM explaining the weaker global trends (Figure 9c,d). In the deep Southern Ocean, the dipolar pattern seen in FREE is reversed in ASM with a warming to the north of the ACC and a cooling to the south (close to Antarctica, Figure 9d). According to Section III.1, this would reflect a strengthening of the Polar front, restricting the cross-frontal mixing.

The relaxation applied in RLX constrains efficiently the air-sea interface, weakens the dipole of warming/cooling and gain of salt/freshening in the Atlantic characterising the model drift and prevent this feature to propagate through the ACC. The relaxation also prevents the shutdown of the AMOC keeping it stable around 8-10Sv (Figure 8). The assimilation has a strong impact on the ocean model in ASM especially in the second part of the century where it reduces the warming trend and allows stronger interannual variability. The assimilation provides stronger intensities and variability in the AMOC than the relaxation (Figure 8), thus enhancing meridional interactions between the water masses in the Atlantic.

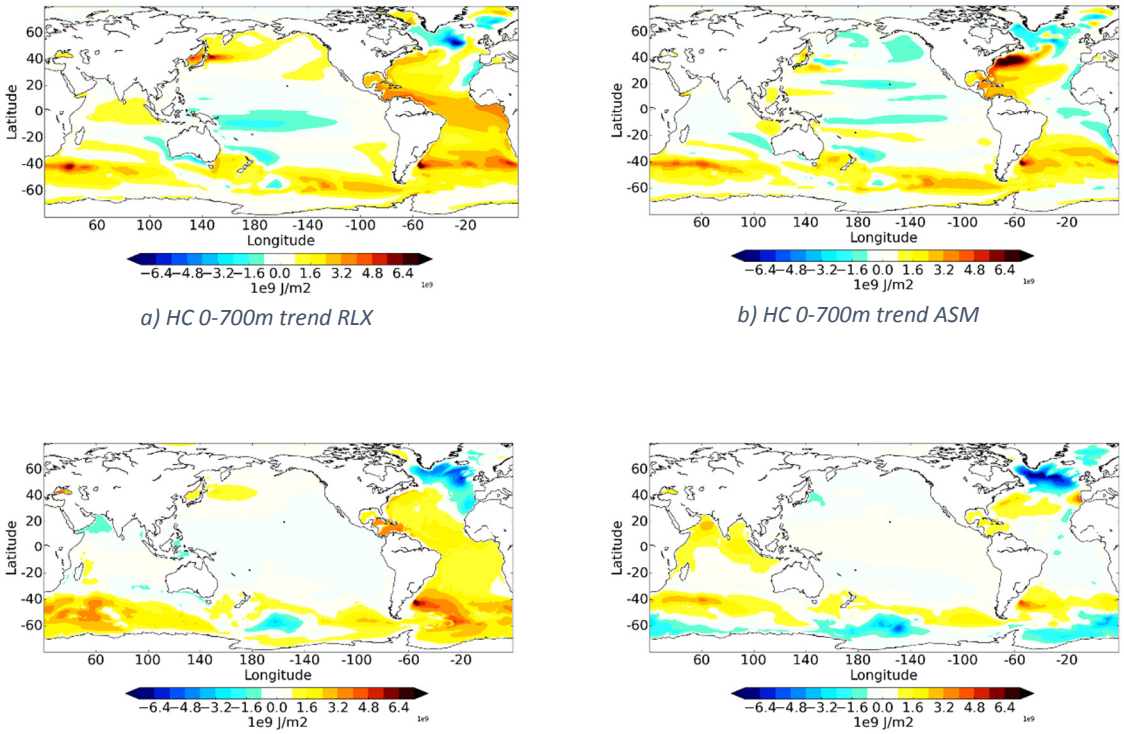

Figure 9 Same as Figure 6 but for the RLX (a,c) and ASM (b,d) runs.

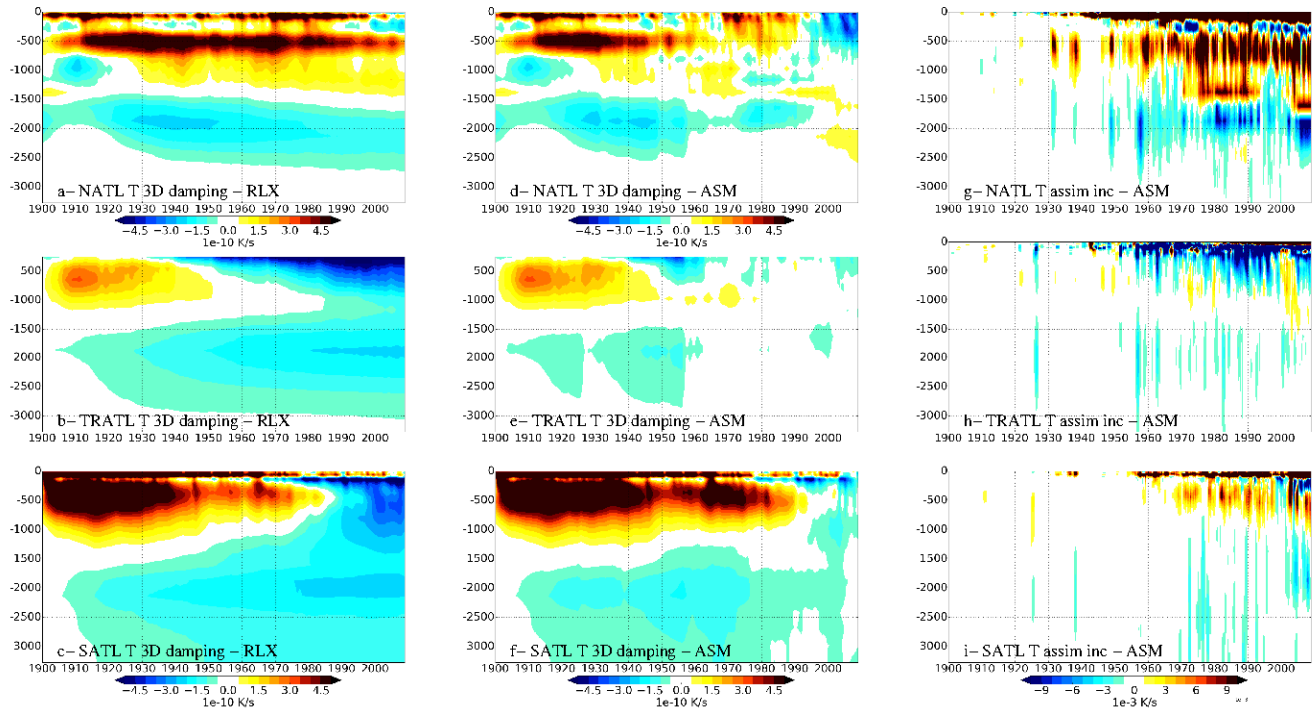

Figure 10 Evolution of the vertical distribution of the 3D temperature relaxation term (in Ks^{-1}) averaged over the North Atlantic, Tropical Atlantic and South Atlantic for the RLX (a,b,c) and ASM (d,e,f) runs. (g,h,i) Same as a,b,c for the temperature assimilation increment (in Ks^{-1}) in ASM.

3. Notes on model drift

If we assume that FREE-CST is uniquely driven by the model drift, subtracting it to FREE will give an estimate of the impact of the variability coming from the atmospheric forcing. It will also give insight into the ability of both the relaxation (RLX) and the assimilation (ASM) to deal with model drift. However, this comparison will not take into account the impact of the internal ocean variability linked to processes such as the AMOC.

The heat contents in ASM and RLX behave similarly in the first part of the century when they are both mainly constrained by the relaxation (Figure 11). While the relaxation reduces the spin-down seen on FREE and the subsequent positive trend in heat content (Figure 5), it does not totally account for the model drift. The ocean heat content in both RLX and ASM indeed shows a positive trend over the period 1910-1950 that is not seen on the "drift-free" FREE-minus-FREE-CST curve. The trend is overall continuous in RLX, confirming the limitations of the relaxation in controlling the model drift. Only the assimilation of observations in ASM is able to stop this positive trend in the 1950s to bring the heat content closer to the "drift-free" behaviour (especially in the upper ocean Figure 11a,b).

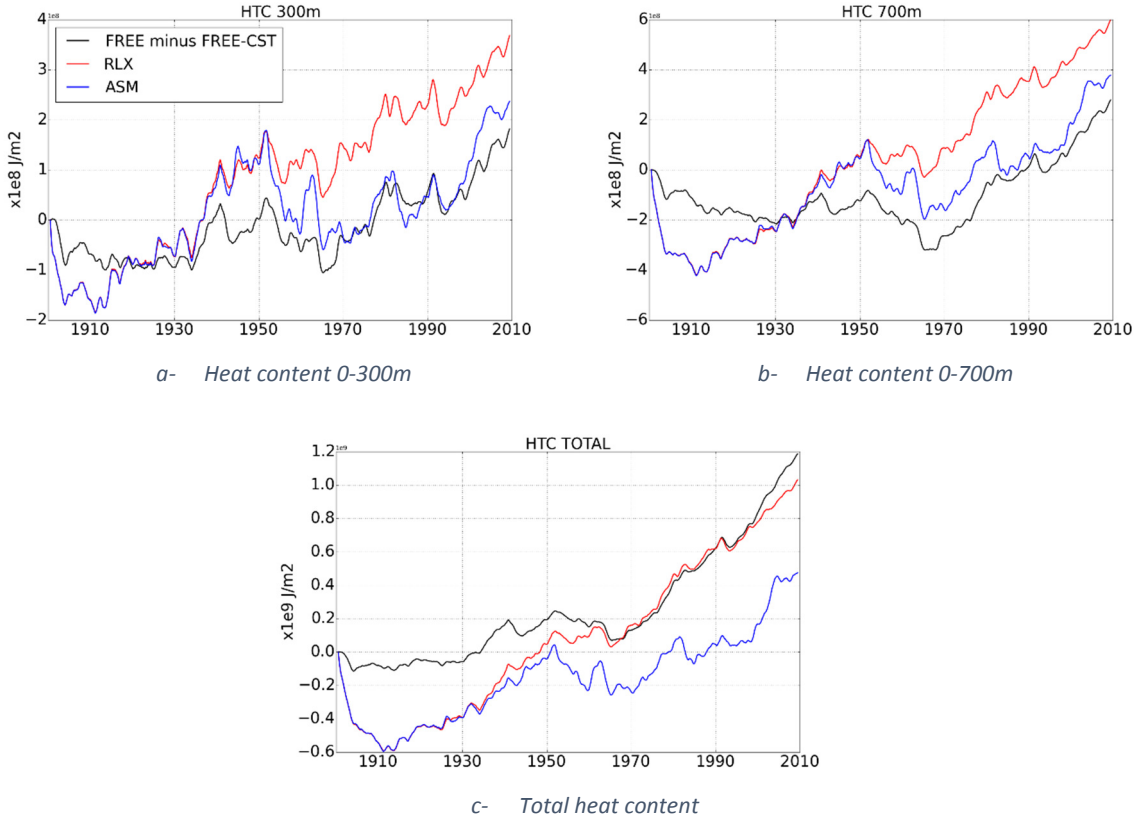

a- Heat content 0-300m

b- Heat content 0-700m

c- Total heat content

Figure 11 Same as Figure 5 but comparing the difference between FREE and FREE-CST with RLX and ASM in terms of model drift. On this Figure, the heat content in RLX and ASM at time t is the difference between the heat contents at time t and t=0.

The trend in upper ocean heat content in FREE-minus-FREE-CST (Figure 12a) shows similar patterns to RLX and ASM (Figure 7a,b) with a warming over the Southern Ocean, in the south and tropical Atlantic, and a dipole in the Nordic Seas. The warming seen in the North Pacific is also visible in RLX.

However the cooling seen in the Tropical Indo-Pacific is seen neither in RLX nor in ASM. Similarly, FREE-minus-FREE-CST does not show the cooling in the Labrador Sea seen in RLX and ASM. These differences suggest that that these aspects of the model drift are not totally controlled by the relaxation in the first part of the century. Part of the differences may also come from internal processes not accounted for by FREE-minus-FREE-CST.

The trend in the deeper ocean in FREE-minus-FREE-CST (Figure 12a) also shows similarities with both RLX and ASM (Figure 7a,b). The warming in the south and tropical Atlantic is more similar to RLX. The warming in the Indian Ocean and the dipolar pattern seen in the Southern Ocean are closer to ASM. These last aspects suggest that the data assimilation has a positive impact on reducing the model drift in those areas. However FREE-minus-FREE-CST never shows the cooling in the Labrador and Nordic Seas seen in both ASM and RLX. As mentioned above, this is likely due to the fact that FREE-minus-FREE-CST does not account for internal ocean processes such as the AMOC that has a significant impact on the heat content trends.

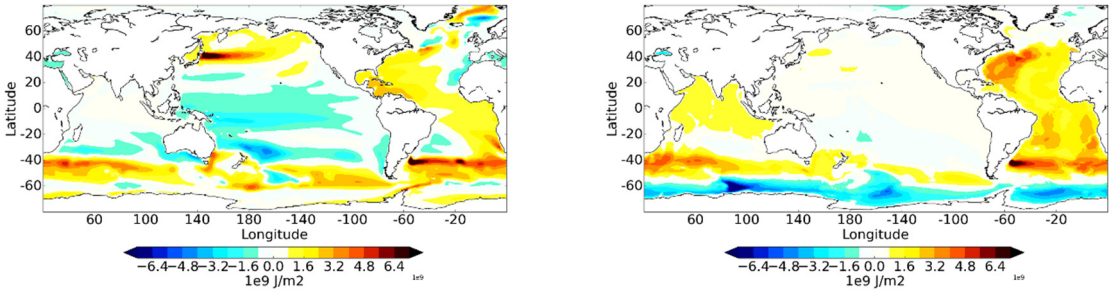

a- HC 0-700m trend FREE minus FREE-CST

b- HC 700-btm trend FREE minus FREE-CST

Figure 12 Same as Figure 7a,c for the difference in heat content between the FREE and the FREE-CST experiments.

IV. Providing initial conditions for a 20th century ensemble ocean data assimilation run

In the previous Section, the model drift and the impact of the relaxation and the assimilation were described in a set of 3 experiments starting from initial conditions from an ORAS4-type run. In this Section, a set of ODA experiments is conducted starting from initial conditions from the RLX run described in Section III.2 (Table 1). The objective is to provide a set of initial conditions for an ensemble ODA that sample probable ocean states for the starting year 1900.

1. Experiment design

The idea behind the data assimilation experiments presented in this Section is to sample the uncertainty in the ocean state in the first part of the 20th century. Three ODA runs (Table 1) are conducted with the same settings as the ASM run and using initial conditions from the RLX

experiment on 1 January 1959. These initial conditions were chosen over other options after showing reduced model spin-up in short ODA experiments (not shown here). The first experiment (ANoBias) is a simple assimilation run over the 20th century while the two others (ABias1 and ABias2) are using bias correction.

The bias correction is the sum of an offline climatological bias correction estimated a priori and of an online correction that depends on the assimilation increment (more details in *Balmaseda et al* [2007] and *Zuo et al* [2015]). The offline bias correction is computed as the monthly climatology of the temperature and salinity assimilation increment from a separate ODA experiment over the well-observed 1989-2009 period. In ABias1, the offline bias correction was estimated from the increments from a 10-day window ODA run forced by ERA-Interim and assimilating EN3 data [*Ingleby and Huddleston*, 2007]. This "old" bias correction is the same as in the ORA-S4 system. In ABias2, the offline term was estimated from the increments from a 10-day window ODA experiment forced by ERA-20C and assimilating EN4 data.

The two estimated bias corrections show different behaviour in the upper 150m (Figure 13a,b). The correction in ABias1 tends to cool the North Pacific and North Atlantic during the summer while the ABias2 correction will warm these regions. Below 150m (Figure 13c,d), the two offline bias correction show similar pattern. The large differences seen close to the surface probably results from the different forcing fields used in the ODA experiments providing the bias correction climatology. Changes in NEMO parameterisations between these experiments (in terms of mixing and active/inactive sea-ice model for example) can also explain part of the differences. Contrary to the temperature offline bias, the offline salinity correction applied to ABias1 and ABias2 show similar patterns in the upper ocean (not shown).

The observations coverage being very poor at the beginning of the 20th century, the offline bias correction will be the major contribution to the total bias correction applied to the ocean. By using different offline bias correction options, we aim to create a wide range of probable ocean states that will be representative of the uncertainty of the beginning of the 20th century.

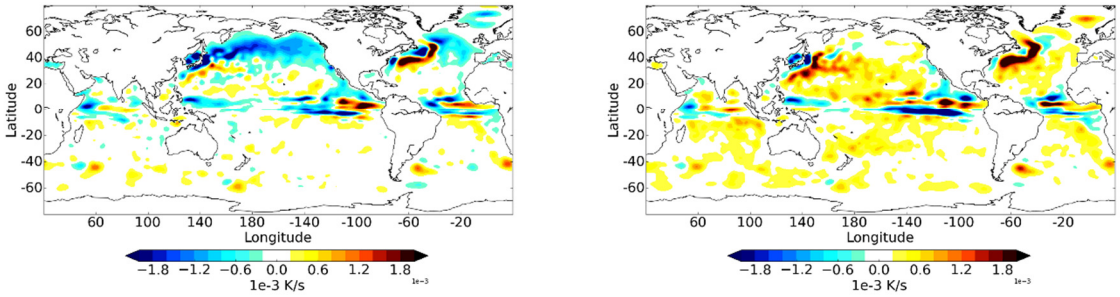

a- 0-150m Tbias ABias1 JJA

b- 0-150m Tbias ABias2 JJA

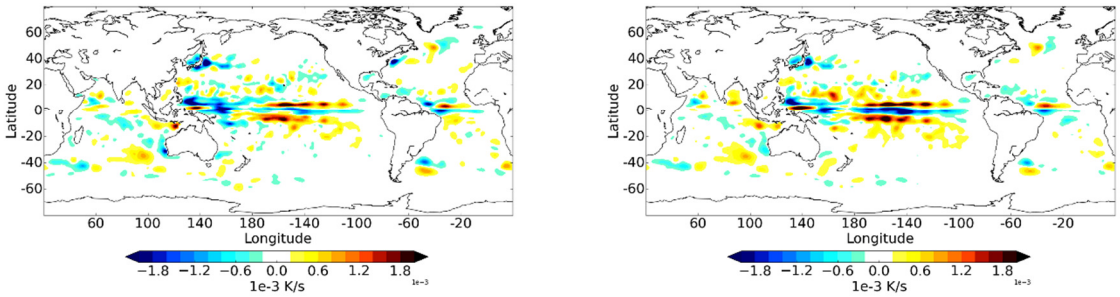

c- 150-300m Tbias ABias1 JJA

d- 150-300m Tbias ABias2 JJA

Figure 13 Offline temperature biases (Ks^{-1}) applied in experiments the layers 0-150m of ABias1 (a) and ABias2 (b) for the JJA season. (c,d) Same as (a,b) but in the layer 150-300m.

2. Increments and bias correction

We first concentrate on what is happening in the North Atlantic Ocean as a result of the bias correction. The temperature assimilation increment in ANoBias increases sharply in the first 100m in the 1950s when the observation coverage starts being decent (Figure 14a). The increase is slightly reduced in ABias1 as the direct bias correction warms the North Atlantic (Figure 14b,d). In ABias2, the increment is considerably reduced (Figure 14c). However, the period from 1940 to 1960 shows substantial negative values followed by a shift to positive values in the late 1960s (Figure 14c). The direct bias correction is warming too much the North Atlantic in the first part of the century (Figure 14e), leading to the sudden response of the increment to bring the system back toward the observed state. This jumpy behaviour of the increment in ABias2 is not a desirable feature for a consistent record.

When looking at the North Pacific, the temperature assimilation increment in ANoBias shows a dipole: a warming of the upper 50-60m and a cooling until 300m depth that increases as the observing system is growing (Figure 15a). In ABias1, the dipolar pattern disappears but is replaced but a strong positive increment in the top 100m resulting from the cool bias correction in this layer (Figure 15b,d). In ABias2, the dipolar pattern is visible but considerably damped with respect to ANoBias (Figure 15c). Values are much weaker than in ABias1 as well, the bias correction pattern in that region being similar to the increment in ANoBias (Figure 15a,e).

Bias correction and increments show contrasted behaviours for the ABias1 and ABias2 experiments according to the location. However, we will see in the next Section that the North Atlantic is a crucial area for the global ocean balance and that the increment seen in ABias2 (Figure 14c) is associated with suspicious dynamical activity that affects the whole Atlantic Ocean.

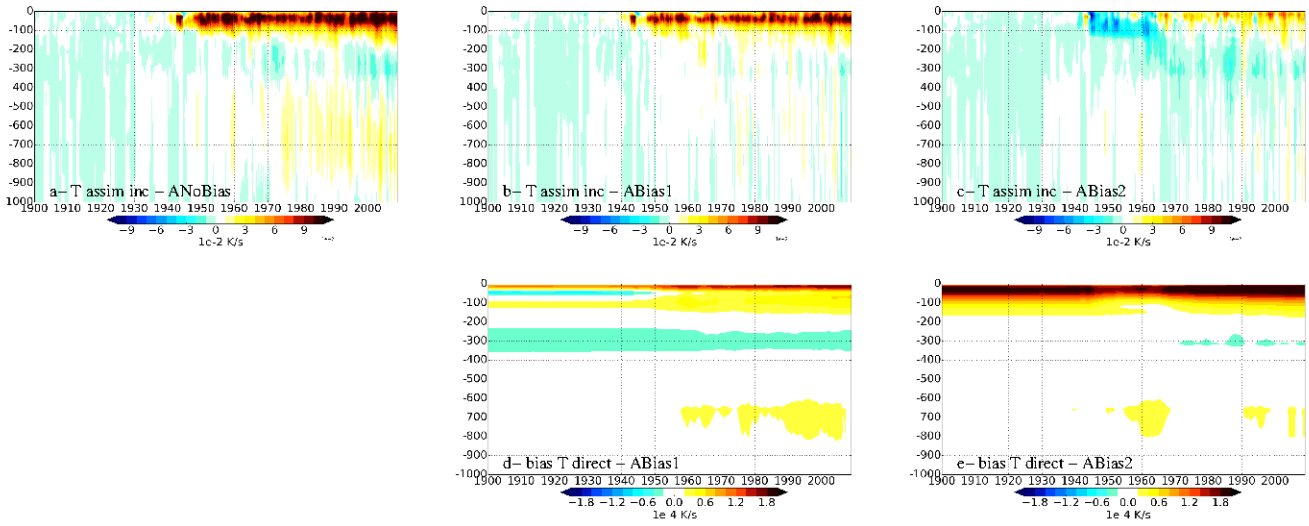

Figure 14 Temperature assimilation increment (Ks^{-1}) averaged over the North Atlantic in ANoBias (a), ABias1 (b) and ABias2 (c). d,e) Direct temperature bias correction (Ks^{-1}) in the same area for ABias1 and Abias2, respectively.

3. Heat content

In the North Atlantic (Figure 16a), the total heat content is relatively stable in ANoBias. In the Tropical Atlantic (Figure 16b), the heat content shows a staircase behaviour, being quite high until the 1950s before dropping in the second part of the century. It seems that the initial state of the ocean is offset from the observed state of the second part of the century in some areas. As soon as the observing system is good enough, the assimilation constrains strongly the ocean giving rise to these staircase behaviours.

The North Atlantic heat content in ABias1 shows a spin-down followed by a strong increase in the 1920s and catches up with ANoBias in the 1950s when the increment becomes substantial (Figure 16a). In the Tropical Atlantic, the heat content start increasing until the 1920s before decreasing in two steps and converging with ANobias (Figure 16b). This change in behaviour between ANoBias and ABias1 is likely the result of the bias correction acting as a catalyst for the AMOC. The AMOC at 26N (Figure 16d) is indeed more intense in ABias1 than in ANoBias in the first part of the century (maximal in the 1930s) increasing the transport of warm water poleward while transferring cool water equatorward at depth. The AMOC modulates the variations of the heat content seen on Figure 16a,b.

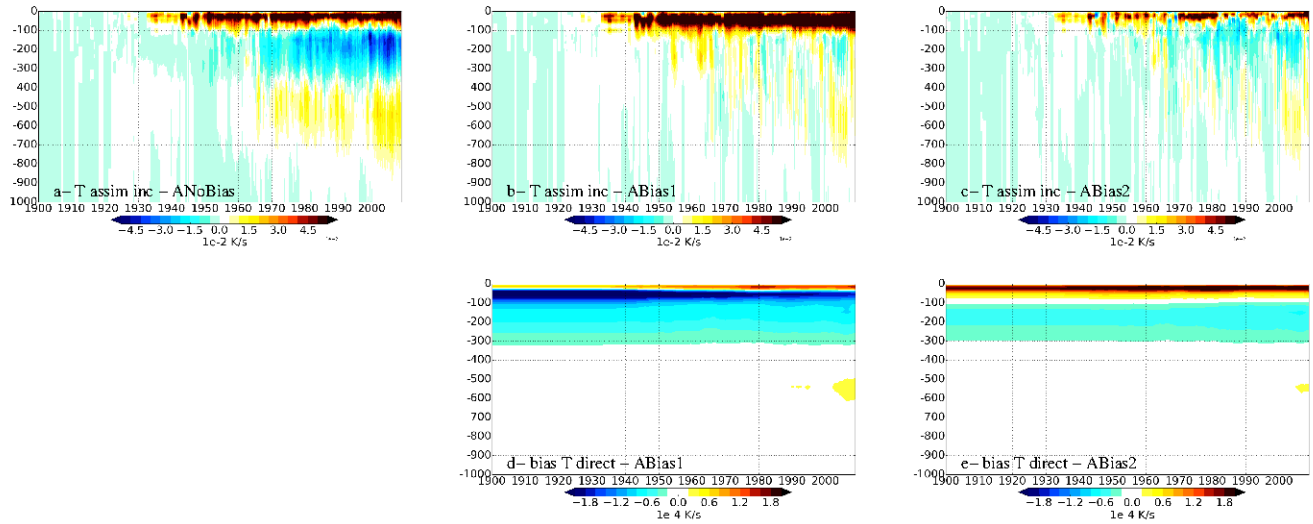

Figure 15 Same as Figure 14 but averaged over the North Pacific.

ABias2 shows a relatively reduced spin-down in North Atlantic heat content followed by a strong increase of the heat content from the 1920s to the 1940s before being constrained by the data assimilation in the last part of the century (Figure 16a). In the Tropical Atlantic (Figure 16b), ABias2 shows a strong decrease in heat content that coincides with the increase reported in the North Atlantic. This strong variations in heat content is related to a very strong AMOC (reaching $30Sv$ in the 1930s, Figure 16d) that greatly intensify the exchange in water masses between the Subpolar and Tropical Atlantic.

One could think that these extreme values for the AMOC make ABias2 a much worse estimate of the ocean state over the century than ABias1. However, the ocean heat content in the North Pacific in ABias1 shows extremely low values and an artificial trend over the century while ABias2 is much more stable and plausible (Figure 16c). Similarly ANoBias looks more conservative but nevertheless shows artificial features (the above mentioned staircases) due to the lack of observations in the first part of the 20th century. The offline bias corrections we apply are only representative of the last decades of the century and are probably not suitable for century-long ocean reanalyses. Other strategies may be considered in the future but, in the following, we decided to remain conservative and to run our ensemble of ODA without bias correction.

In spite of their respective limitations, ANoBias, ABias1 and ABias2 provide a good variety of possible ocean states for the early 20th century that will be used as initial conditions for a 10-member ensemble ODA over the 20th century.

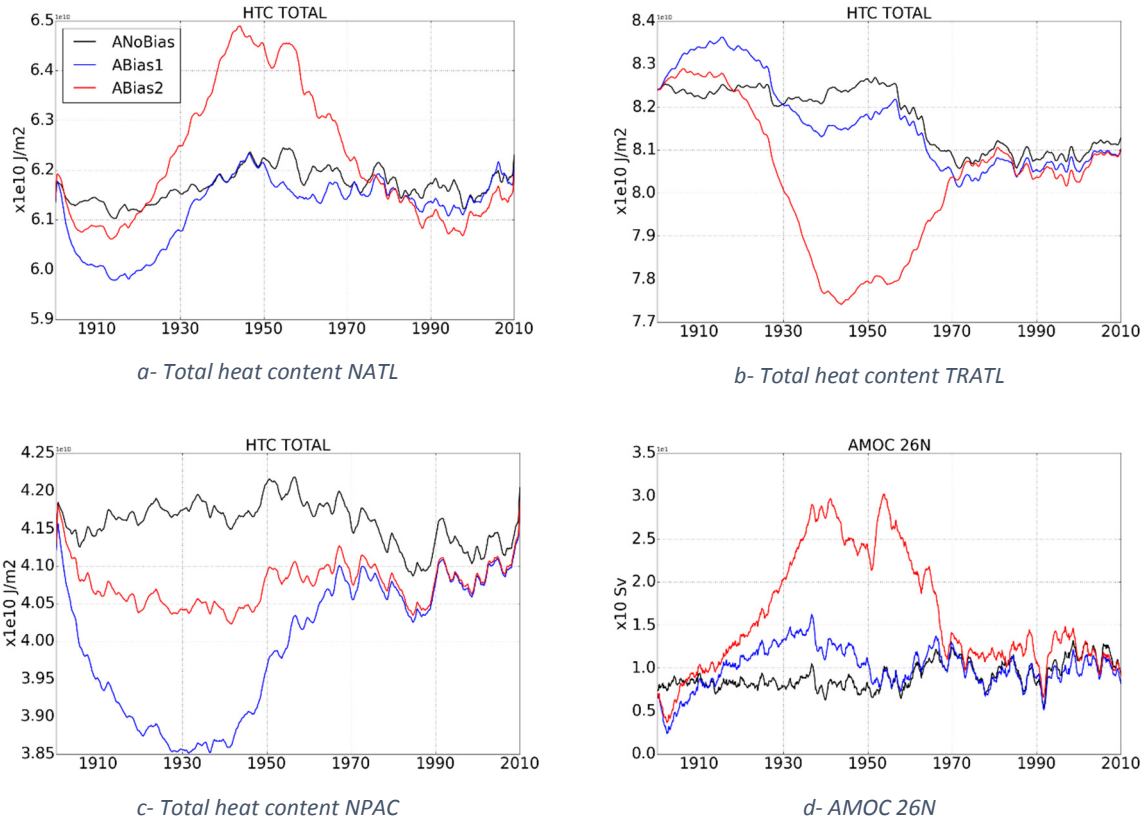

a- Total heat content NATL

b- Total heat content TRATL

c- Total heat content NPAC

d- AMOC 26N

Figure 16 Evolution of the total ocean heat (in Jm^{-2}) in the North Atlantic (a), Tropical Atlantic (b) and North Pacific (c). The ANoBias experiment is in black, ABias1 in blue, and ABias2 in red. (d) AMOC at 26N (in Sv)

V. ORA-20C: an ensemble of ocean data assimilation over the 20th century

1. Experiment design

ORA-20C is a 10-member ensemble of ocean data assimilation over the 20th century (1900-2009) that uses the same NEMO and NEMOVAR configurations as the ASM run described in Section II.2. As a reminder, ORA-20C is forced by the ERA-20C deterministic run, uses a SST relaxation, a weak 3D relaxation to climatology and assimilates EN4 temperature and salinity profiles (Table 1). Additionally, ORA-20C uses perturbations on SST, sea-ice concentration (*Hirahara et al.* [2016]), surface fluxes and ocean observations [*Zuo et al*, In preparation]

The 10 initial conditions for ORA-20C are chosen from selected ocean states in ANoBias, ABias1 and ABias2. These provide uncertainty for the state of the ocean on 01-01-1900. Ocean states from 01-01-1936, 01-01-1940, 01-01-1951 and 01-01-1959 are selected in ANoBias and ABias1. As we saw in the previous Section that ABias2 showed some suspicious features, only two ocean states from 01-01-1930 and 01-01-1965 are selected from this experiment.

2. General behaviour of ORA-20C

In this Section, the general behaviour of ORA-20C is analysed through different aspects. When possible it is compared to other ocean analysis products. ORAS5 is the ¼˚ resolution ocean reanalysis with 75 vertical levels (ORCA025Z75) currently produced over the period 1975-present at ECMWF. A 1˚ resolution and 42 levels (ORCA1Z42) experiment has also been conducted and will be used for comparison with ORA-20C. This experiment is 5-member ensemble of ODA and is referred to as ORAS5-like. Along with the EN4 temperature and salinity profiles, the Hadley Centre provides a monthly objective analysis (referred to as EN4OA) on a 1˚ regular grid and on the same 42 vertical levels as ORCA1Z42. The SODA 2.2.4 reanalysis [*Carton and Giese*, 2008] (referred to as SODA) is an ODA experiment conducted over the period 1871-2010 using 20CRv2 atmospheric forcings [*Compo et al*, 2011] and assimilating temperature and salinity from the World Ocean Database 2009 [*Boyer et al,* 2009]. A monthly average mapped onto a regular ½˚ grid and 40 vertical level has been made available and is used for intercomparisons. EN4OA and SODA are only used for the heat content comparisons.

a. Ocean heat content: comparison with other products

The upper (0-300m) ocean heat content in ORA-20C is very similar to the ORAS5-like experiment over the 1975-2010 period (Figure 17a). It is no big surprise as the two systems are very close and well constrained by observations at that period and for this depth range. In the layer 0-700m (Figure 17b), the agreement is still good despite some noticeable differences in the 1970s. Considering the full column (Figure 17c), ORA-20C shows similar interannual signals to ORAS5-like but a larger long-term warming trend.

ORA-20C shows substantial differences with SODA and EN4OA in the early 20th century. When the observation coverage is good enough, all the products converge and show similar interannual variability signals. The convergence speed depends on the observation coverage and on how far off ORA-20C and SODA are from the EN4OA mean state. The warming trend in the first 300m is on average stronger in SODA (Figure 17a). When considering thicker layers, the long-term variability in SODA is much closer to EN4OA than in ORA-20C that shows overall stronger long-term variability (Figure 17b,c). Discriminating by latitudinal bands (extratropics and tropics) confirms that the global view (see Supplementary materials).

This difference in long-term variability is likely to depend on several aspect. ORA-20C could be more realistic but larger long-term trends and some staircase behaviours suggests the presence of some model drift suddenly constrained by the data assimilation in the 1950s. The relatively low variability in SODA is probably linked to the way the model is constrained to profiles but also to climatology for the deep layers (below 1000m) over the 20th century.

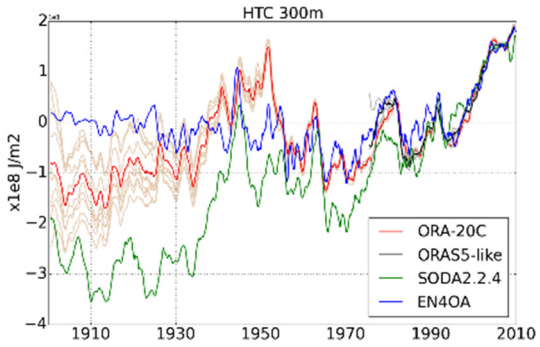

a- Global heat content 0-300m

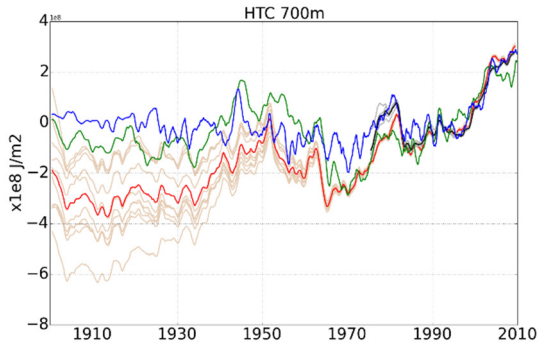

b- Global heat content 0-700m

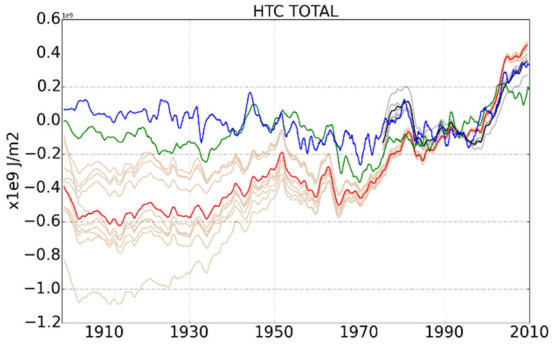

c- Global heat content - full column

Figure 17 Global (60˚S/60˚N) ocean heat content (Jm^{-2}) anomalies with respect to EN4OA average over 1970-2000 for a) the layer 0-300m, b) the layer 0-700m and c) the total column . ORA-20C ensembles are in light red, ORA-20C ensemble mean in red, ORAS5-like ensembles in grey, ORAS5 ensemble mean in black, SODA2.2.4 in green and EN4OA in blue.

b. Atlantic ocean: heat content and AMOC

When looking at ORA-20C heat content timeseries, one soon realises that the lack of observations in the first part of the century leaves the ocean model in ORA-20C trying to reach its own equilibrium (Figure 18). Focusing on the North, Tropical and South Atlantic basins, the total heat content in ORA-20C shows a large spread in the first half of the 20th century (Figure 18a,b,c) that rapidly decreases in the following decades as the temperature increments become larger (Figure 18e). Some members show very similar behaviour to the ANoBias experiment over the century with coinciding features of variability. There seems to be two outliers among the ensemble members that start with high (low) heat contents in the North (Tropical) Atlantic. These two members are starting from initial conditions taken from ABias2. When looking at the AMOC at 26˚N (Figure 18d), the outliers show high intensities in the first years of the run before converging towards the rest of the ensembles. By 1910, all the members show a similar AMOC that matches the one from ANoBias. The AMOC is then quite flat until the assimilation enhances and modulates it in the second part of the century. The heat content evolution in the Atlantic suggests that ORA-20C is relying mainly on the ocean model in the first part of the century. As the observing network is growing, the increments get larger (Figure 18e) and the assimilation strongly constrains the ocean state, dramatically reducing the ensemble spread.

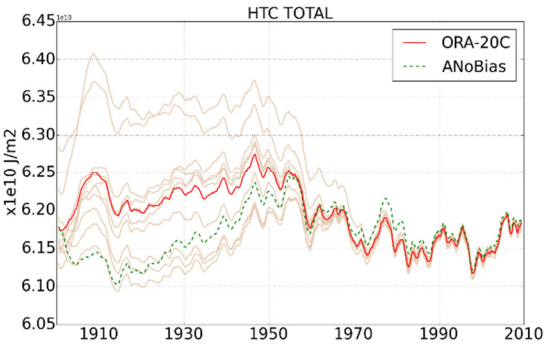

a- Total heat content NATL

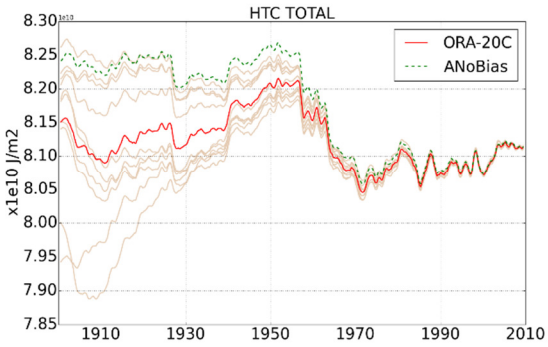

b- Total heat content TRATL

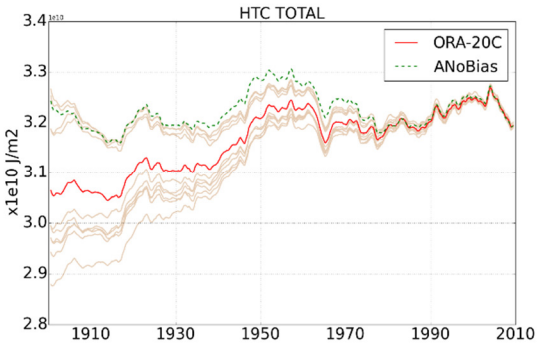

c- Total heat content SATL

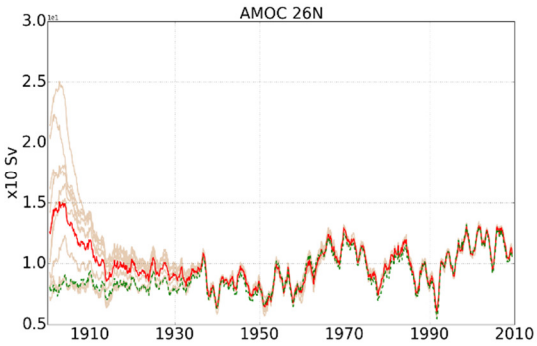

d- AMOC at 26˚N

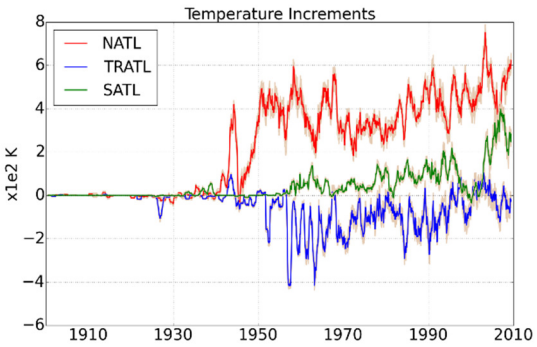

e- Temperature increments 0-300m

Figure 18 Evolution of the total ocean heat (in Jm^{-2}) content in the North Atlantic (a), the Tropical Atlantic (b) and the South Atlantic (c). ORA-20C ensembles are in light red and the ensemble mean in red. ANoBias is the dashed green line. (d) AMOC at 26N (in Sv). d) Temperature increments (in K) averaged over the layer 0-300m in the North Atlantic (red), the Tropical Atlantic (blue) and the South Atlantic (green)

c. Sea level and sea-ice thickness

ORA-20C provides timeseries of the global sea-level (Figure 19a), a parameter considered as an essential climate variable. It can be compared to a certain extent to the reconstruction that *Church et al.* [2011] conducted from satellite and in-situ observations only. As for the heat content, the spread in sea level is quite large at the beginning of the century and is greatly reduced as the observation coverage gets better. Depending on the ORA-20C member, the early 20th century is a

mixture of steady and slowly decreasing or increasing sea-level. On average, the trend is slightly positive around $0.2\ mm/year$. From the 1950s to the mid-1960s, the sea-level shows a decrease with a trend around 0.5mm/year. While the trend is indeed relatively slow from the early-1900s to 1930 in *Church et al* [2011] (lower than 1mm/year), the sea level rise is steady afterwards with trends from $1.8 \pm 0.3\ to\ 2.8 \pm 0.8\ mm/year$. The FREE experiment shows a similar pattern of weak positive trend before a steady rise, suggesting that the weak trend in the first part of the century in ORA-20C is resulting from the relaxation trying to limit the model drift. Similarly the decrease in sea level seen in the middle of the timeseries is likely linked the data assimilation bringing the system closer to observations and thus disturbing the response of the model to the forcing. From the mid-1960s to the 1990s, the sea level in ORA-20C is again increasing very slowly. From the 1990s to the end of the record, the sea levels rises by around $2\ mm/year$, which is closer to *Church et al* [2011]'s $2.8 \pm 0.8\ mm/year$. ORA-20C shows similar trends to ORAS5-like over their overlapping period (1975-2009).

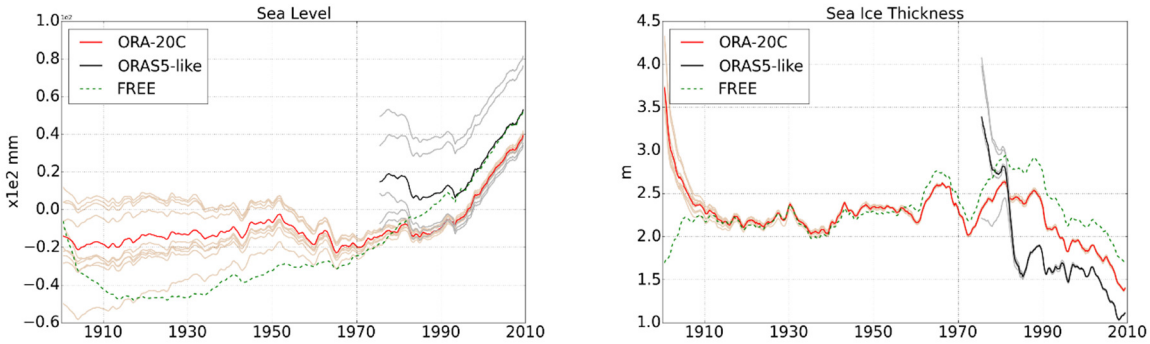

a- Global sea level *b- Arctic sea-ice thickness*

Figure 19 a) Global sea level in mm. b) Sea ice thickness (in m) in the Arctic. ORA-20C ensembles are in light red, ORA-20C ensemble mean in red, ORAS5-like ensembles in grey, ORAS5 ensemble mean in black and FREE is in dashed green

ORA-20C also provides sea-ice conditions from LIM2 over the 20th century. Here we focus on the sea-ice thickness in the Arctic (Figure 19b). ORA-20C ensembles start from initial conditions coming from experiments assimilating the sea-ice from HadISST2, which showed unrealistic sea-ice thickness in the Arctic. It takes around 15 years to ORA-20C to come back to a more reasonable sea-ice thickness (close to the FREE experiment). From there on, the Arctic sea-ice thickness stays quite steady between 2 and 2.5m up the mid-1960s. It hen shows a larger variability until the 1980s where the sea-ice thickness starts a continuous decrease from 2.5m to less than 1.5m in 2010. The comparison with FREE suggests that the interannual variability comes mainly from the atmospheric forcing, while the values of the thickness seem to be affected by the data assimilation after the 1960s. The late 20th century decreasing trend in ORA-20C can be seen in ORAS5-like from the mid-1980s with lower thickness values. This melting of the Arctic sea ice matches the trend seen in other ECMWF ocean reanalyses and observational products as shown in *Tietsche et al* [2014].

VI. Summary and conclusion

The main purpose of conducting a 20th century ensemble of ODA such as ORA-20C is to provide ocean initial states for the streams of CERA-20C within the ERA-CLIM2 project. But the work done for ORA-20C goes beyond this sole objective and provides insights on how the ocean model behaves in a long term run and how it responds to ERA-20C atmospheric forcing and the changes in observing system when assimilating data. ORA-20C is also the first ensemble of 20th century ocean reanalyses conducted at ECMWF.

The main challenge in 20th ocean experiments is to cope with the uncertainty about the ocean state at the beginning of the 20th century. The first ocean experiments, with and without ODA shows that the model responds by a spin down/up and then a drift toward a model climate. The AMOC collapses to very low values in the first part of the century. The reasons for such model behaviour are still not fully understood. It is however well known that the mixing scheme in this NEMO configuration is too intense, leading to more transfer of heat and salt from the surface to the subsurface. The role of the sea-ice model in such behaviour needs to be investigated as this component could have a substantial impact in the ECMWF coupled reanalysis system and on the CERA-20C product.

The relaxation to SST, the weak 3D constraint to climatology and the assimilation work to limit the spin down/up and the drift of the ocean model. The relaxation dominates in the first part of the century while the assimilation is the major constraint toward observations from the 1950s onwards. Both components enhance the AMOC allowing more meridional exchanges of water masses. The transition from the poorly observed early 1900s to the post-1950s period can be the source of discontinuities in the ocean record. Investigations are needed to find a more consistent way to constrain the ocean model for century-long ODA.

The offline bias correction computed from ODA experiments forced by ERA-20C is very different from the one computed in the past for ORAS4-type experiments forced by ERA-Interim. The different NEMO configuration and forcing fields are likely to explain such differences. The presence of the sea-ice model could also be a reason as the signal is particularly strong in the North Atlantic and the North Pacific.

Bias corrected ODA experiment trigger adjustments in the ocean dynamics and thermohaline properties characterised by an intensification of the AMOC and its variability. These adjustments are particularly obvious in the early 20th century when the offline term dominates. The bias correction can have positive impact by reducing the size of the increments in some regions. But it can also have the opposite effect and/or induce jumps that make it unsuitable for a consistent 20th century ODA. Such jumps are seen at the transition between poor and good observation coverage as the increment thrives to constrain the model toward observations. Research toward a better suited bias correction may be an answer to the issues of consistency due changes in the observing system.

The ODA experiments with/without bias correction provide a variety of probable ocean states for 1900 that are used to initialise the 10 members of ORA-20C. ORA-20C shows a strong spread at the beginning of the century. The lack of observations leaves the ocean model attracted toward its own climate until the assimilation really kicks in after the 1950s. In the last part of the century ORA-20C shows very little spread and a good agreement with other reanalysis products (such as ORAS5 and SODA2.2.4) as well as observations.

The transition from a relatively free model to a constrained system makes the 20th century record of the state of the ocean from ORA-20C difficult to rely onto for the study of climate signals. Contamination is visible in most of the ocean basins except in well-constrained regions like the upper North Atlantic. Similar issues are seen in the SODA2.2.4.

The ocean initial conditions for the streams of CERA-20C that started at the end of 2015 comes from the 10 ORA-20C members. The ocean component from CERA-20C uses the same NEMO configuration as ORA-20C but the atmospheric forcing are passed through the ECMWF coupled system. A continuous monitoring of CERA-20C is being carried out with respect to ORA-20C to detect the impact of the coupling on the ocean and the assimilation system.

REFERENCES

Balmaseda, M. A., Dee, D., Vidard, A. and Anderson, D. L. T. (2007), A multivariate treatment of bias for sequential data assimilation: Application to the tropical oceans. Q.J.R. Meteorol. Soc., 133: 167–179. doi: 10.1002/qj.12

Balmaseda, M. A., Mogensen, K. and Weaver, A. T. (2013), Evaluation of the ECMWF ocean reanalysis system ORAS4. Q.J.R. Meteorol. Soc., 139: 1132–1161. doi: 10.1002/qj.2063

Balmaseda, M. A., K. E. Trenberth, and E. Källén (2013), Distinctive climate signals in reanalysis of global ocean heat content, Geophys. Res. Lett., 40, 1754–1759, doi:10.1002/grl.50382.

Boyer, T. P., et al. (2009), World Ocean Database 2009, vol. 1, Introduction, NOAA Atlas NESDIS, vol. 66, edited by S. Levitus, 219 pp., NOAA, Silver Spring, Md.

Breivik, Ø., K. Mogensen, J.-R. Bidlot, M. A. Balmaseda, and P. A. E. M. Janssen (2015), Surface wave effects in the NEMO ocean model: Forced and coupled experiments, J. Geophys. Res. Oceans, 120, 2973–2992, doi:10.1002/2014JC010565.

Compo, G. P., and co-authors, 2011, The Twentieth Century Reanalysis Project. Q.J.R. Meteorol. Soc., 137: 1–28. doi: 10.1002/qj.776

Good, S. A., M. J. Martin and N. A. Rayner, 2013. EN4: quality controlled ocean temperature and salinity profiles and monthly objective analyses with uncertainty estimates, Journal of Geophysical Research: Oceans, 118, 6704-6716, doi:10.1002/2013JC009067.

Hersbach, H., Peubey, C., Simmons, A., Berrisford, P., Poli, P. and Dee, D. (2015), ERA-20CM: a twentieth-century atmospheric model ensemble. Q.J.R. Meteorol. Soc., 141: 2350–2375. doi: 10.1002/qj.2528

Hirahara, S., Balmaseda, M., de Boisséson, E., Hersbach, H., 2016. Sea Surface Temperature and Sea Ice Concentration for ERA5. ERA Report Series. In preparation.

Ingleby, B., and M. Huddleston, 2007, Quality control of ocean temperature and salinity profiles - historical and real-time data. Journal of Marine Systems, 65, 158-175 10.1016/j.jmarsys.2005.11.019

Laloyaux, P., Balmaseda, M., Dee, D., Mogensen, K. and Janssen, P. (2016), A coupled data assimilation system for climate reanalysis. Q.J.R. Meteorol. Soc., 142: 65–78. doi: 10.1002/qj.2629

Levitus, S., et al. (2012), World ocean heat content and thermosteric sea level change (0–2000 m), 1955–2010, Geophys. Res. Lett., 39, L10603, doi:10.1029/2012GL051106.

Mogensen, K., M. Alonso Balmaseda, A. Weaver, 2012. The NEMOVAR ocean data assimilation system as implemented in the ECMWF ocean analysis for System 4. ECMWF Technical Memoranda No 668, February 2012

Poli, P. and co-authors, 2015, ERA-20C Deterministic, ERA report series No.20.

Poli, P. and co-authors, 2016, ERA-20C: An atmospheric reanalysis of the 20th century, J. of Climate, In revision.

Tietsche, S., M. Alonso Balmaseda, H. Zuo and K. Mogensen, 2014, Arctic sea ice in the ECMWF MyOcean2 ocean reanalysis ORAP5. ECMWF Technical Memoranda No 737, October 2014

Zuo, H., Balmaseda, M. and Mogensen, K., 2015, The ECMWF-MyOcean2 eddy-permitting ocean and sea-ice reanalysis ORAP5. Part1: Implementation. ECMWF Technical Memoranda No 736, February 2015

Supplementary materials

A. Salt content in spin-up experiments

The behaviour of the salt content is more difficult to understand than the heat content but it can bring useful information for the understanding of the model drift.

As for the heat content (see Section III.1, Figure 5), the global salt content in FREE-CST and FREE spins down to reach a low plateau in the 1910-1930s and, below 700m, starts drifting with a positive trend (Figure 20). Differences between the 1910-1930 and the 1980-2000 periods are computed. From the surface (Figure 21a,b) to the bottom (Figure 22), the salt content decreases in the North Atlantic and increases in the Equatorial and South Atlantic in a very similar fashion in both FREE-CST and FREE. Below 700m (Figure 22c,d), the ocean gains salt south of the deep ACC matching the hypothesis of the mixing across the weak Polar Front. The loss of salt in the deep Indian Ocean and in the southeastern Atlantic follow the shape of the Indian gyre and corresponds to the cooling seen on Figure 7g,h. The dipole in the Atlantic basin matches what happens with the ocean heat content and the FREE-CST experiment results suggests that the model drift is responsible for most of it.

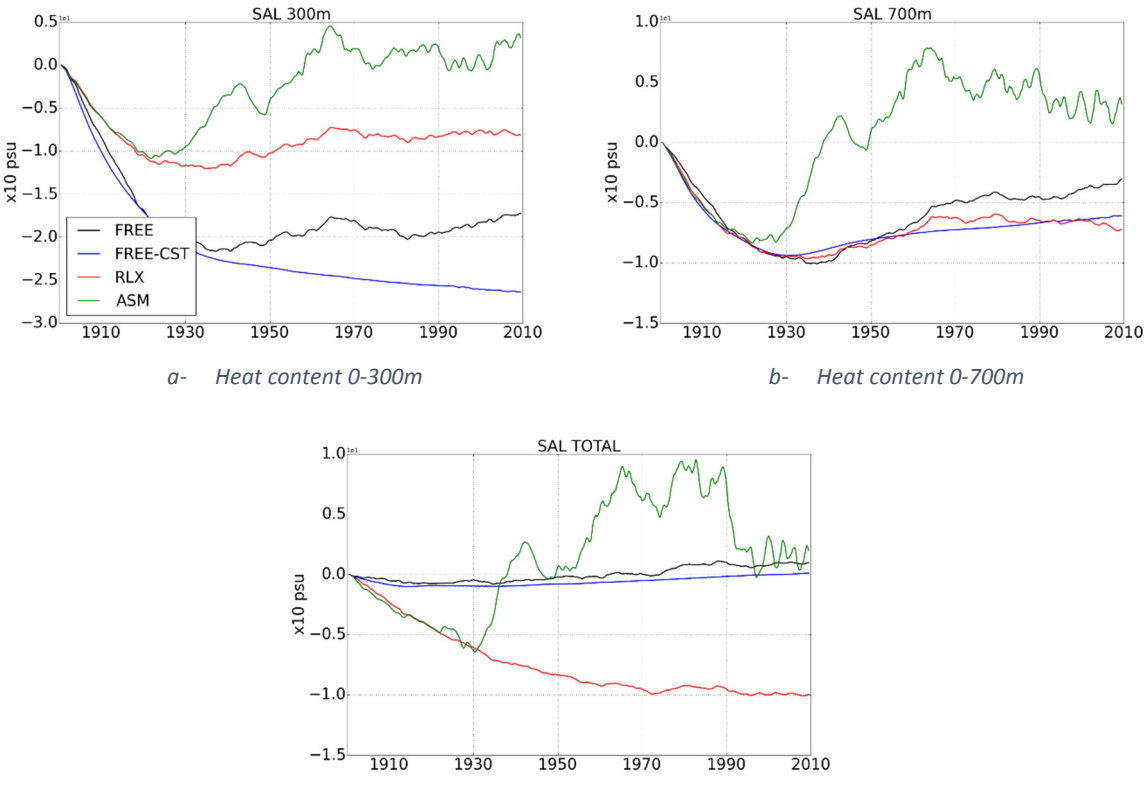

a- Heat content 0-300m

b- Heat content 0-700m

c- Total heat content

Figure 20 Evolution of the salt content (in psu m) with respect to the initial condition for a) the 0-300m layer, b) the 0-700m layer and c) the whole water column in experiments FREE (black), FREE-CST (blue), RLX (red) and ASM (green).

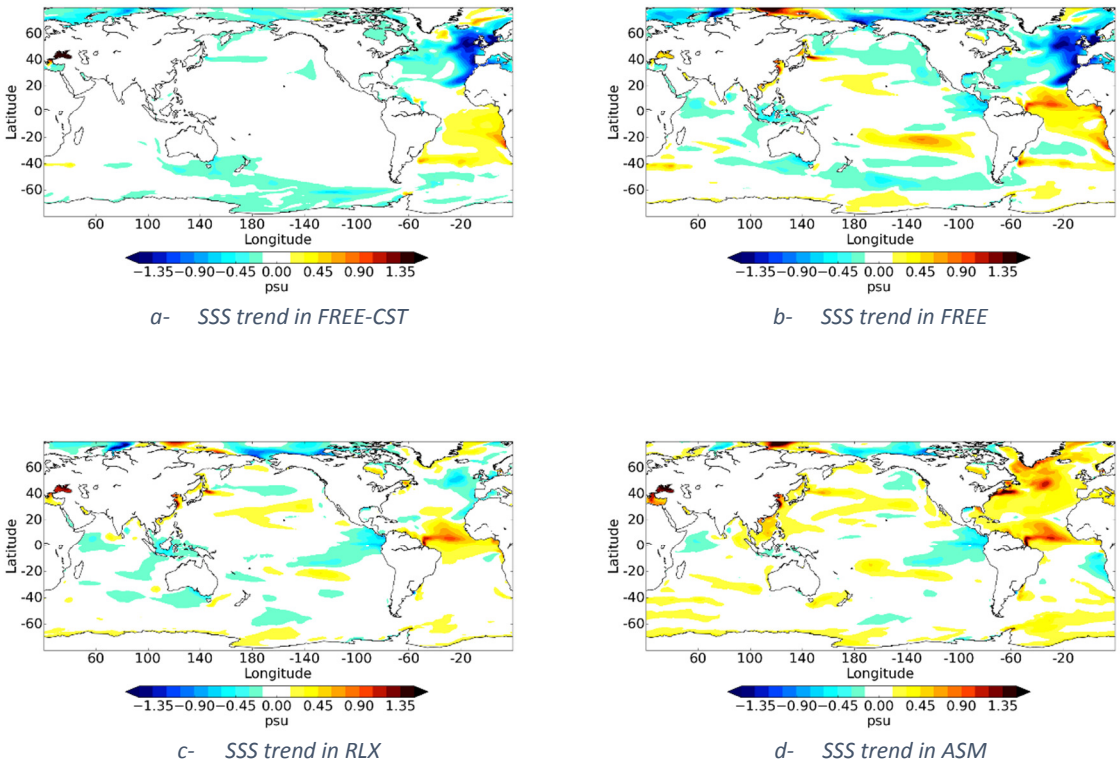

a- SSS trend in FREE-CST

b- SSS trend in FREE

c- SSS trend in RLX

d- SSS trend in ASM

Figure 21 Difference between the periods 1980-2000 and 1910-1930 in SSS (in psu) in experiments a) FREE-CST, b) FREE, c) RLX and d) ASM.

The salt content in RLX shows a much weaker spin down than FREE in the 0-300m layer (Figure 20a). It reaches a low in 1910-1930 and then increases with a similar trend as FREE to reach a plateau by the 1970s. In the 0-700m (Figure 20b), RLX and FREE show similar spin-down followed by an increase but RLX stabilises from the 1970s onwards while FREE continues drifting. Considering the full column (Figure 20c), RLX decreases continuously while FREE remains quite stable. The SSS in RLX shows less freshening than FREE in the northeast Atlantic while keeping a similar gain of salt in the Equatorial Atlantic off the Amazon estuary (Figure 21c). In deeper layers (Figure 23a,c), the dipolar pattern in the Atlantic basin is weakening. This weakening is mainly due to the 3D relaxation adding salt in the upper North Atlantic and freshening the subsurface of the Tropical Atlantic as shown on Figure 24a,b,c. Below 700m, RLX shows a substantial freshening in the subpolar Atlantic that is not compensated by a similar gain of salt (Figure 23c).

In ASM, the global salt content increases rapidly from the 1930s to reach a new level by the 1960s that is actually quite close to the FREE run when considering the whole column (Figure 20). The SSS show a large positive trend off the Amazon estuary, similar to what is seen in RLX (Figure 21c,d). The SSS trend is also substantially positive in the subpolar Atlantic. In the subsurface, the dipolar pattern in the Atlantic Ocean seen in the other experiments has disappeared as a result of the combination of the relaxation in the first part of the century and the increment from the 1950s onwards (Figure 24d,e,f,g,h,i) that are adding salt in the North Atlantic and freshening the Tropical Atlantic. The substantial increase in salt content over the Gulf Stream area (Figure 23b) coincides with the increase in heat content seen on Figure 9b. In the deep ocean, the freshening in the subpolar Atlantic in RLX is slightly reduced in ASM (Figure 23d).

The trend in salt content in the different experiments confirms that both the relaxation and the data assimilation act to reduce the model drift by mainly enhancing the AMOC and allowing more meridional exchange of water masses in the Atlantic Basin (Figure 8).

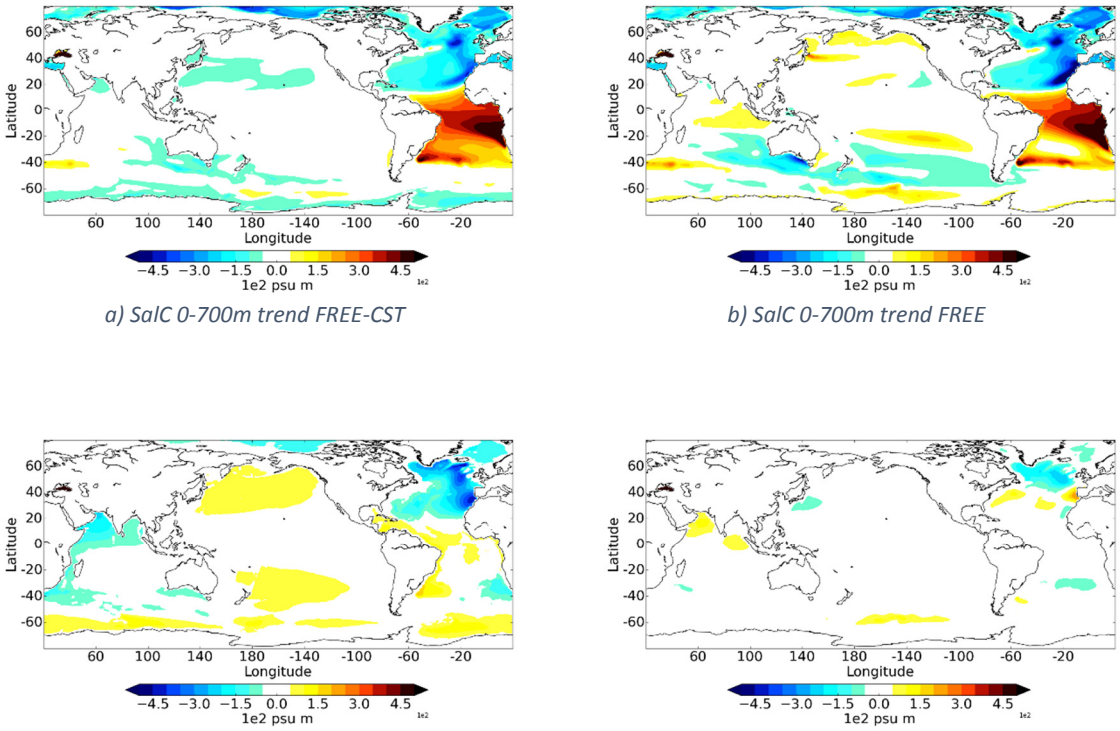

a) SalC 0-700m trend FREE-CST

b) SalC 0-700m trend FREE

c) SalC 700-btm trend FREE-CST

d) SalC 700-btm trend FREE

Figure 22 Difference between the periods 1980-2000 and 1910-1930 in a,b) salt content (in psu m) for the 0-700m layer, c,d) heat content for depths below 700m for the FREE-CST and the FREE experiments, respectively.

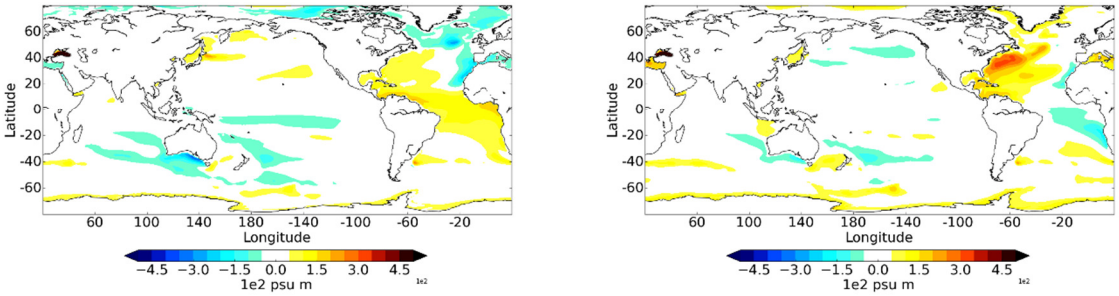

a) SalC 0-700m trend RLX

b) SalC 0-700m trend ASM

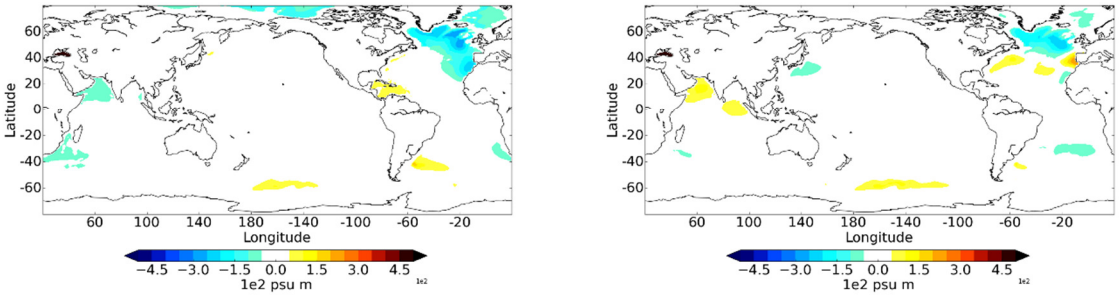

c) SalC 700-btm trend RLX

d) SalC 700-btm trend ASM

Figure 23 Same as Figure 22but for experiments RLX (a,c) and ASM (b,d).

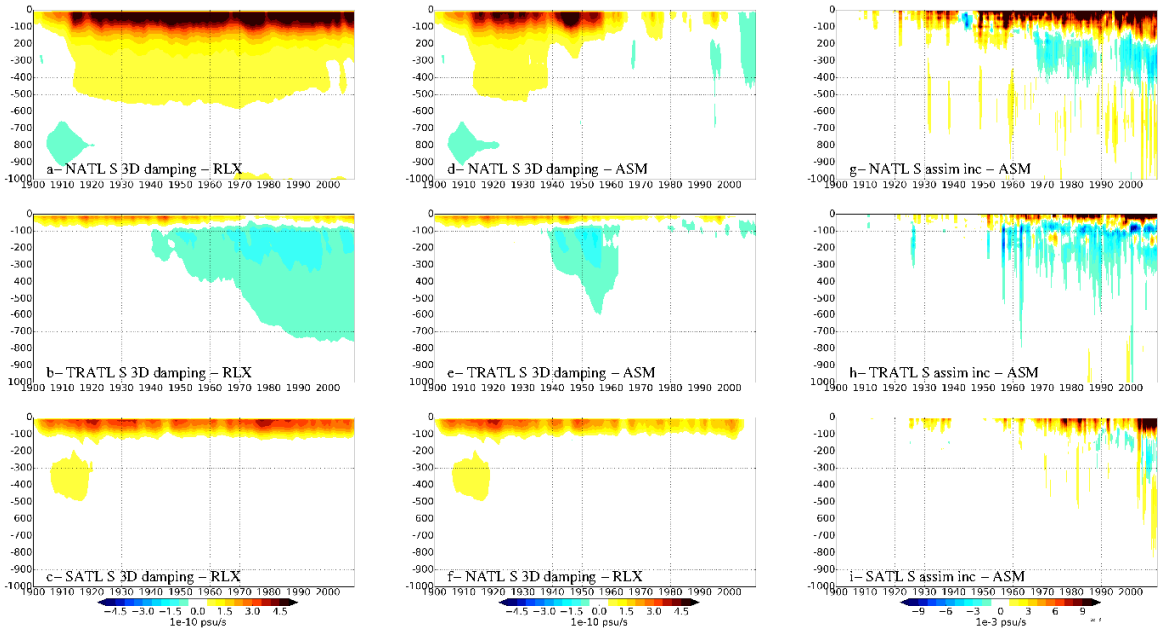

Figure 24 Same as Figure 10 but the salinity relaxation (in $psu\ s^{-1}$, a,b,c,d,e,f) and increment (in $psu\ s^{-1}$, g,h,i).

B. Heat content comparisons: area averages

In Section V.2.a, we compared the global heat content from ORA-20C with ORAS5-like, SODA and EN4OA. Here we separate the domain in three latitudinal bands distinguishing the northern/southern extratropics and the Tropics.

The upper ocean in the northern extratopics (Figure 25a,b) is relatively well constrained by the observations from the 1950s onwards with ORA-20C and SODA converging toward EN4OA. The deeper layers of ORA-20C (Figure 25c) converge toward EN4OA only from the late 1970s. At those depths, observations are very scarce and the constraint applied on the ocean is very weak. SODA is particularly close to EN4OA at depth (Figure 25b,c) and show less long term variability than ORA-20C, suggesting a relatively strong constraint to observations.

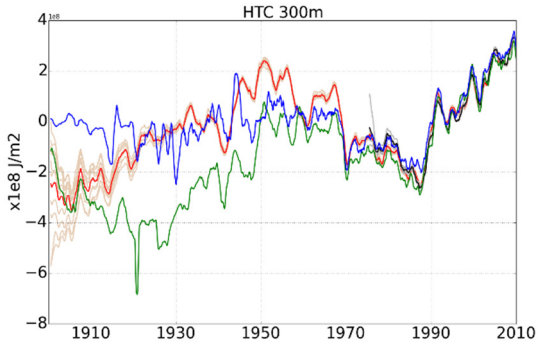

a- Heat content 0-300m Northern extratropics

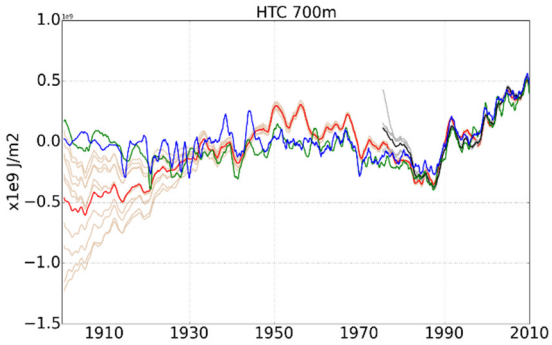

b- Heat content 0-700m Northern extratropics

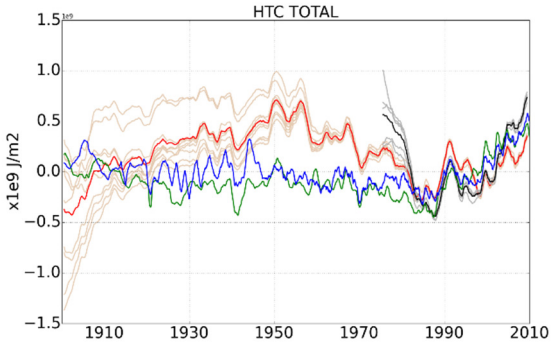

c- Total heat content Northern extratropics

Figure 25 Ocean heat content (Jm^{-2}) anomalies in the Northern extratropics (30˚N/70˚N) with respect to EN4OA average over 1970-2000 for a) the layer 0-300m, b) the layer 0-700m and c) the total column . ORA-20C ensembles are in light red, ORA-20C ensemble mean in red, ORAS5-like ensembles in grey, ORAS5 ensemble mean in black, SODA2.2.4 in green and EN4OA in blue.

In the Tropics, the upper ocean (Figure 26a) shows different trends for ORA-20C and SODA. The heat content in ORA-20C is relatively high and stable in the first part of the century. By the 1960s, it decreases sharply to be stable again up to the 2000s and then increases until 2010. SODA has a relatively low heat content that increases progressively to converge towards ORA-20C and EN4OA by the mid-1970s. Considering the 0-700m layer (Figure 26b), ORA-20C is remarkably close to EN4OA during the whole period while SODA still shows a warming trend. The total heat content in ORA-20C

and SODA is on average very similar in the Tropics (Figure 26c) and converges towards EN4OA by the 1980s. This suggests that different vertical distribution of heat in ORA-20C and SODA in the Tropics, likely to be due to their respective model characteristics.

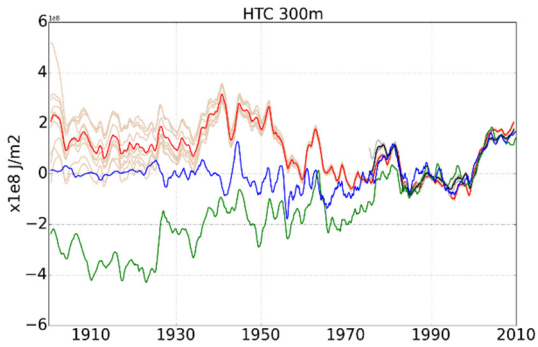

a- Heat content 0-300m Tropics

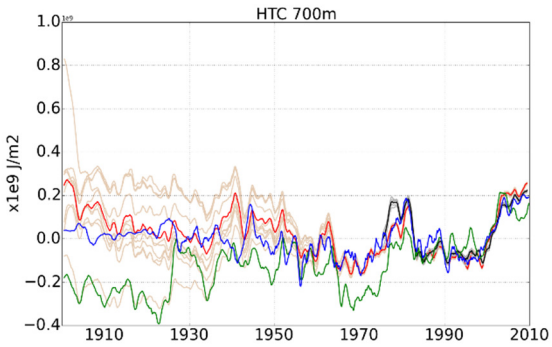

b- Heat content 0-700m Tropics

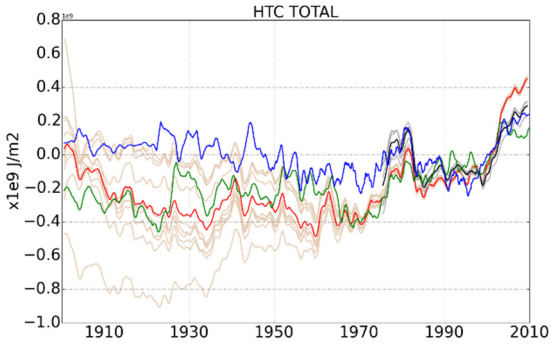

c- Total heat content Tropics

Figure 26 Same as Figure 25 for the Tropics (30˚S/30˚N).

In the Southern extratropics, the observation coverage is relatively low. The heat content in ORA-20C shows a long term warming trend before converging toward EN4OA by the 1980s when the observation coverage starts to be decent (Figure 27a,b,c). SODA does not show any obvious long term trends and stays relatively close to EN4OA, suggesting a significant constraint to climatology. SODA also shows a strong sensitivity to either the forcing or the data assimilation (or both) with two peaks in heat content coinciding with the two World Wars.

Overall, in both products, the data assimilation is playing a very important role in constraining the ocean state. The first part of the century highlights the real differences between the two systems that are due to model specification, initialisation, data assimilation methods and handling of the transition from the poorly to the well observed periods.

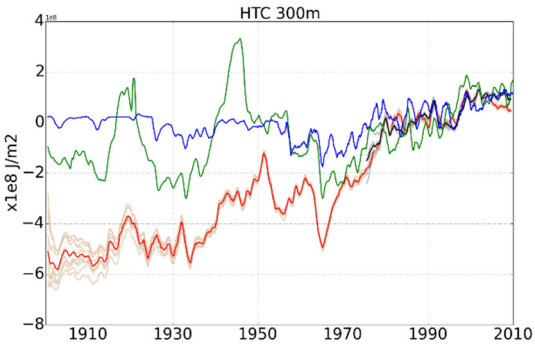

a- Heat content 0-300m Southern extratropics

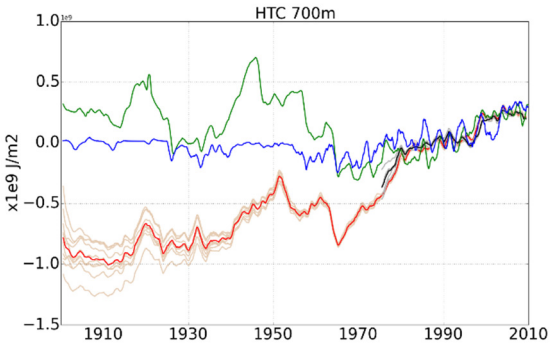

b- Heat content 0-700m Southern extratropics

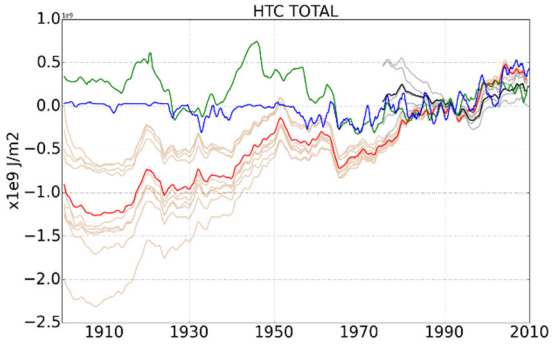

c- Total heat content Northern extratropics

Figure 27 Same as Figure 25 for the Southern extratropics (30˚S/70˚S).